

Part IV

Scanning Probe Microscopy

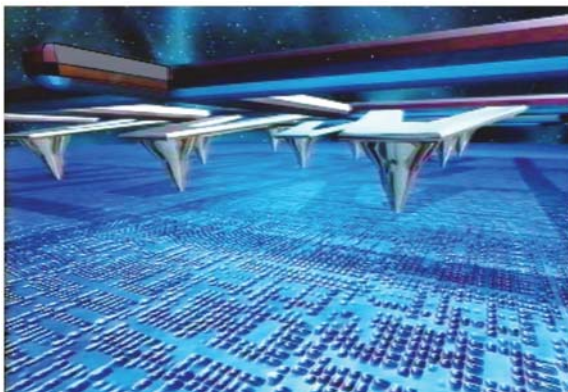
Chapter X: Scanning Probe Microscopy

G. Springholz - Nanocharacterization I

Chapter 10

Scanning Probe Microscopy

Basic Principles, Tip-Sample Interactions, Scan Modes



Contents Chapter 10:

Scanning Probe Microscopy

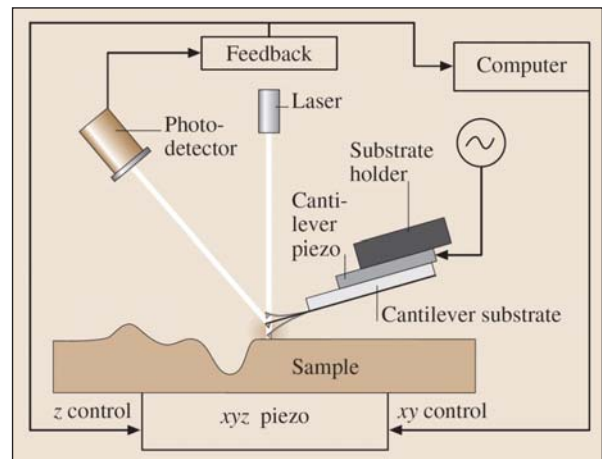
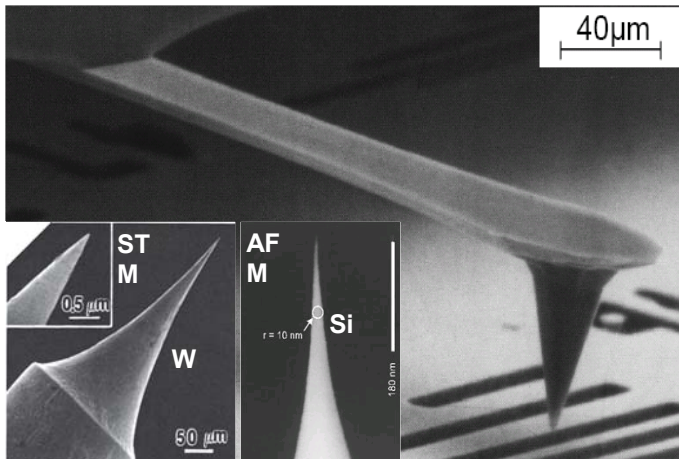
10.1 Introduction.....	1
10.2 Features of Scanning Probe Microscopy.....	4
10.2.1 Resolution and Contrast	4
10.2.3 In situ and in vivo SPM	6
10.2.4 Nanomanipulation and Nanopatterning using SPM	7
10.2.5 Miniaturization.....	9
10.3 Probe-Sample Interactions.....	10
10.3.1 Mechanisms Contributing to the Tip-Sample Interaction.....	11
10.3.2 Other Tip-Sample Interactions	12
10.4 The Tunnelling Current: STM	14
10.4.1 Quantum Mechanical Description of the Tunneling Process.....	15
10.4.2 Consequences for the Lateral Resolution of STM.....	17
10.5 Force Interactions and Force Detection: AFM	18
10.5.1 Microscopic and Macroscopic Forces	18
10.5.2 Force Sensors: Micromechanical Cantilevers	22
10.5.3 Cantilever Design.....	23
10.5.4 Measurement of the Cantilever Beam Deflection.....	28
10.6 Comparison: Atomic Resolution in AFM / STM	30

10.7 Piezo Scanners	32
10.7.1 The Piezoelectric Effect	34
10.7.2 Displacement for a Piezo Plate due to Applied Voltage	35
10.7.3 Tube Scanner	37
10.7.4 Flexure Scanner (x,y).....	39
10.8 Imaging Strategies and Scan Modes	40
10.8.1 Constant Height Mode	41
10.8.2 Constant Interaction Mode.....	42
10.9 Feedback Loop and Scan Control	44
10.9.1 Feedback Control Action.....	46
10.9.2 PID Feed-Back Controller	47
10.10 Non-Contact / Tapping Mode AFM.....	54
10.10.1 Cantilever as Driven Damped Harmonic Oscillator	55
10.10.2 Oscillating Cantilever Interacting with a Sample Surface.....	56
10.10.3 Oscillation Detection Modes: Amplitude versus Frequency Detection	59
10.10.4 Intermittent Contact (Tapping) versus Non-Contact Mode.....	60
10.10.5 Comparison of the different AFM Imaging Modes.....	61
10.11 AC-Modulation or Dynamic Scan Modes	62
10.12 Hybrid Scan Modes.....	65
10.13 Multi-Pass Methods	71
10.14 Summary	74
Appendix	76
Literature.....	77
History of Scanning Probe Microscopy	78

10.1 Introduction

Scanning Probe Microscopy (SPM)

- ❖ Group of **microscopic techniques** in which the **sample surface is scanned** with a needle-like, i.e., **microscopically sharp probe tip kept** at a distance of 0 - 50 Å away from the surface.
- ❖ Local information on the sample properties is obtained by measuring different kinds of **tip-sample interactions**. Their strength depends on the **tip-sample distance** and allows to control with a sub-Ångström precision.
- ❖ Keeping the interaction strength constant during raster scanning of the sample surface by using a feed-back loop, the **3D surface topography** can be **quantitatively** determined.

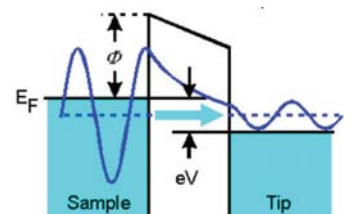
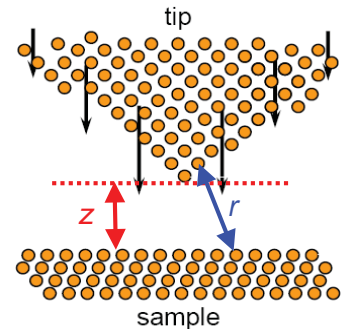
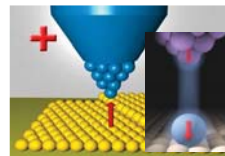


Variants of Scanning Probe Microscopy Techniques

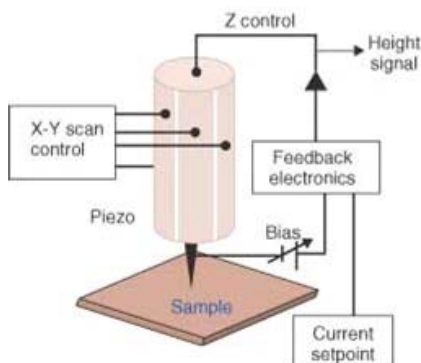
Many **different variants of SPM techniques** exist. These are distinguished by (i) which **kind of tip-sample interaction** is measured during the scanning process and (ii) what detection scheme is used for measurement for the interaction.

Main techniques:

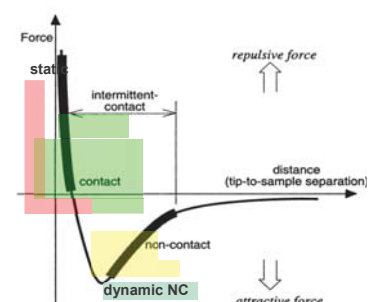
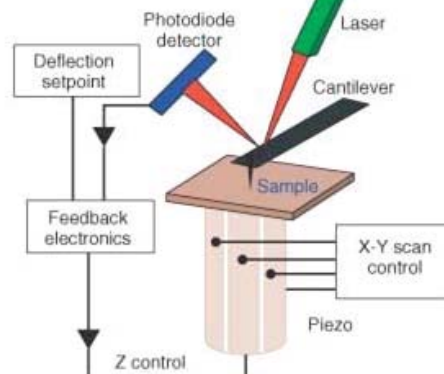
Scanning Tunneling Microscopy (STM),
Scanning (Atomic) Force Microscopy (SFM/AFM),
Scanning Near Field Optical Microscopy (SNOM).



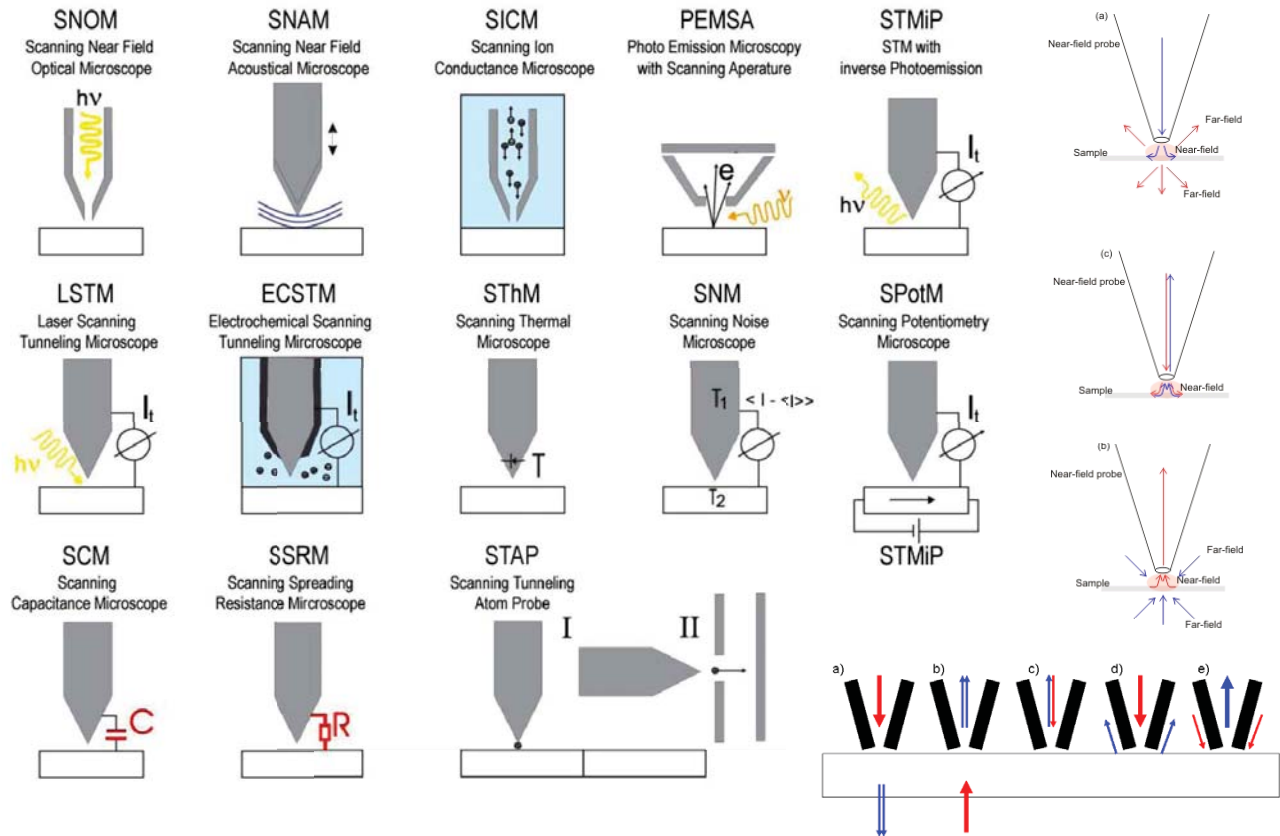
Scanning Tunneling



Atomic Force Microscopy



.. by measuring different interactions signals during the scanning process



10.2 Features of Scanning Probe Microscopy

10.2.1 Resolution and Contrast

- ❖ SPM microscopy yields unprecedented sub-Å vertical and lateral resolution ("true atomic resolution"), which is much better than any other method.

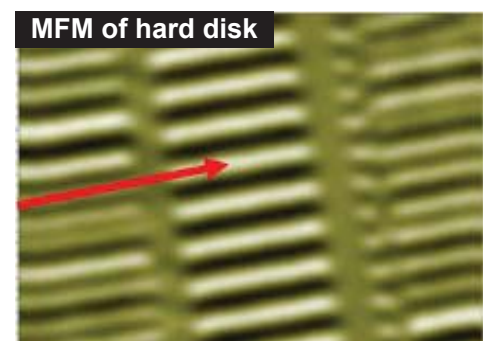
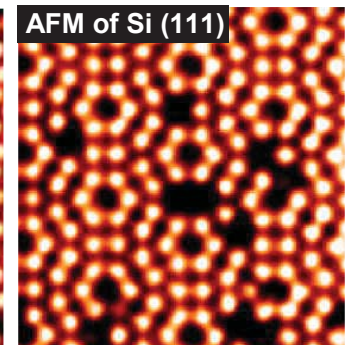
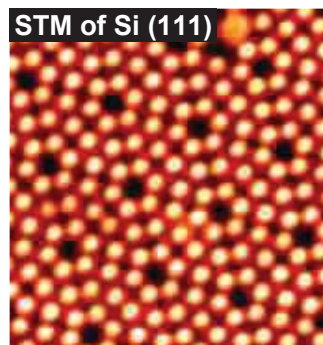
» Allows **direct imaging** of the **real atomic structure** of surfaces.

Resolution limits: No longer determined by diffraction effects but by the **tip-sample interaction length**, **noise level**, as well as by the **sharpness** (radius and shape) of the **SPM tip**.

Routinely achieved: $\Delta z \sim 0.3 \text{ Å}$, $\Delta x \sim 1 \text{ Å}$ (STM) and $\sim 5 \text{ Å}$ (AFM). **Best:** $\Delta z \sim 0.02 \text{ Å}$, $\Delta x \sim 0.1 \text{ Å}$.

- ❖ **Image contrast:** Depends on the type of tip – sample interaction detected and recorded during the scanning process. Example (left): Magnetic structure of hard disk.

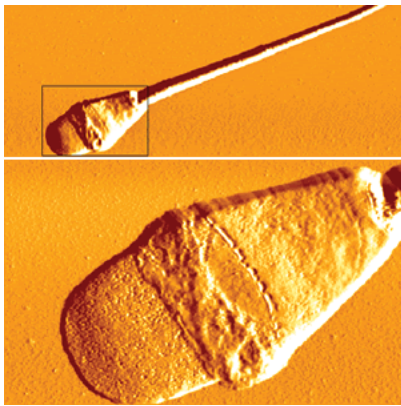
- ❖ **Spectroscopy** (=measurement of the interaction strength versus distance, applied voltage, etc.), as well as different **scan modes** can be used to obtain particular information on the local sample properties such as magnetic, electronic, mechanical properties, etc.



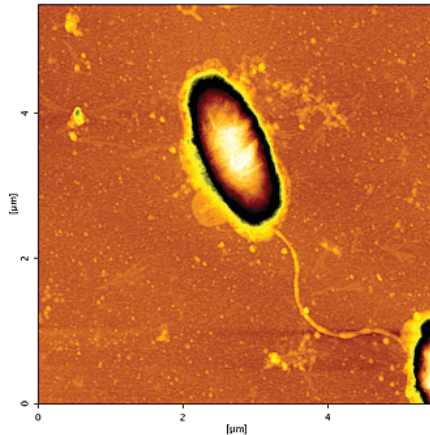
10.2.2 Additional Features

- ❖ SPM allows investigation of various **local chemical, physical and biological properties** at **specific surface sites** by fixing the tip at a certain position and recording spectroscopy data.
Examples: Measurement of local density of states, frictional, magnetic, electrical properties.
- ❖ **No or negligible sample damaging** occurs during imaging. This allows imaging of soft biological specimen and other soft materials and structures (organic structures, polymers, etc.).
- ❖ **No special sample preparation** is required at least for AFM that may alter the sample.

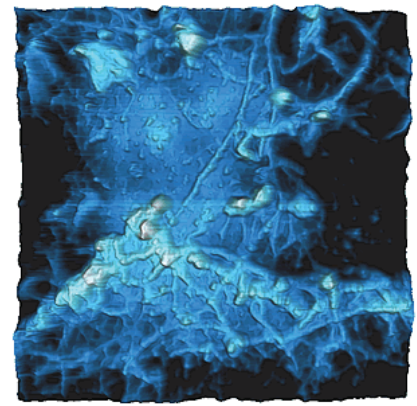
Example for SPM images of biological specimen:



Deflection images of sperm imaged in PBS solution. Scan range 40µm (top), 11µm (bottom)



Bacterial cell (H. pylori) in air



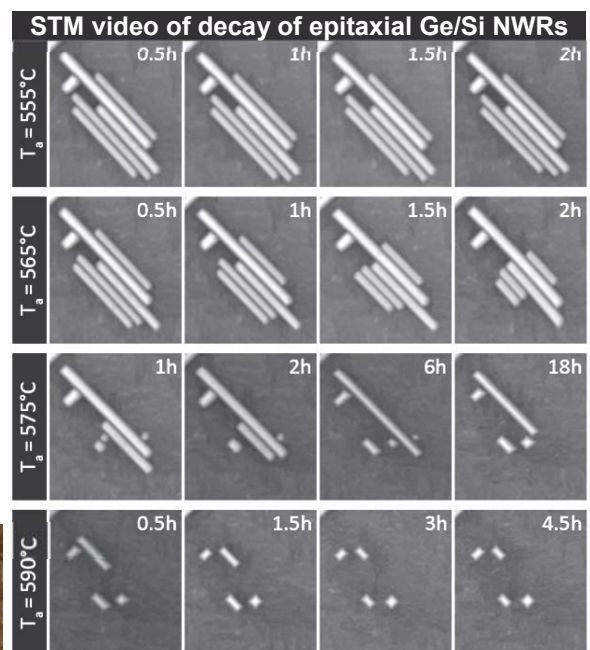
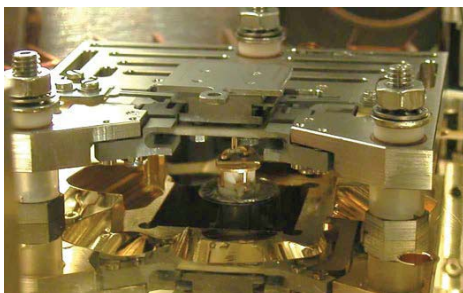
Fibrenetwork in a protein cement in buffer
Scan range 6 µm * 6 µm

10.2.3 In situ and in vivo SPM investigations

SPM microscopy can be performed under many different environmental conditions (air, gases, liquids, vacuum, high/low temperature, ...). Thus, it can be employed to study **in vivo** the **dynamics of surfaces** and biological systems **in real time**.

Examples: Study of adatom diffusion (hopping), aggregation, surface phase transitions, growth, etc. .

Limitation: Limited time resolution due to limited scanning speed of the SPM tip. Typical image recording times are of the order of minutes/image. Fast scanning systems may achieve acquisition times of several seconds per image.

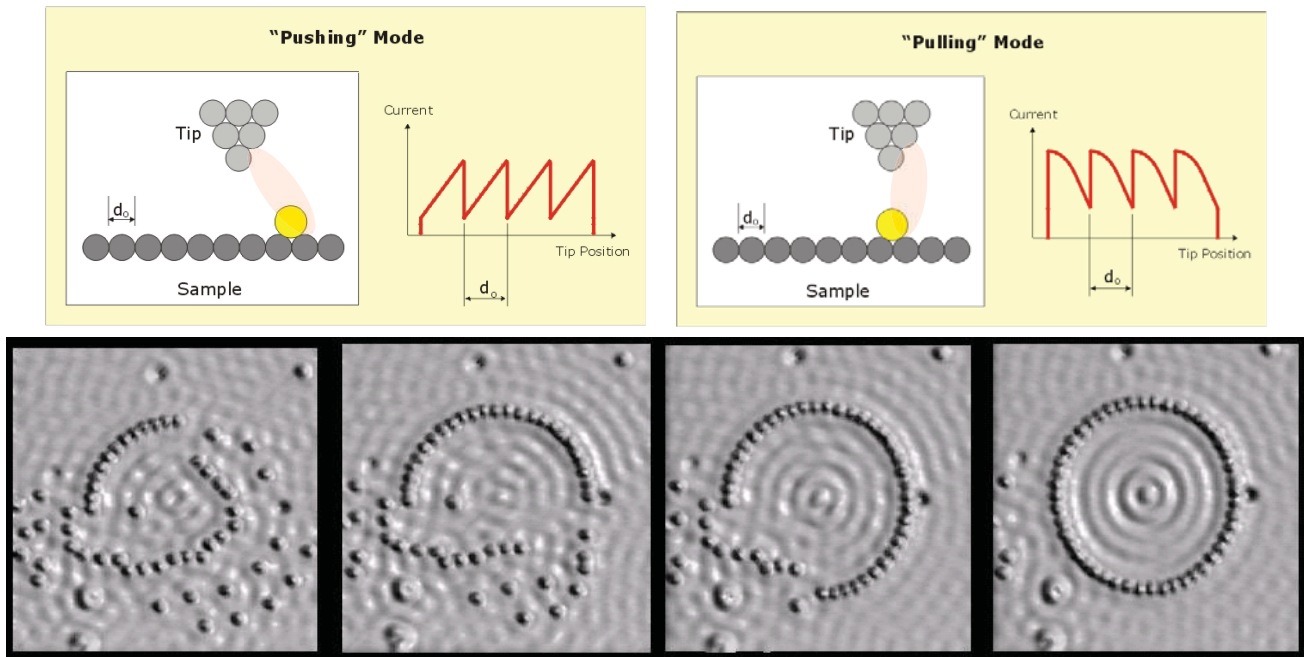


10.2.4 Nanomanipulation and Nanopatterning using SPM

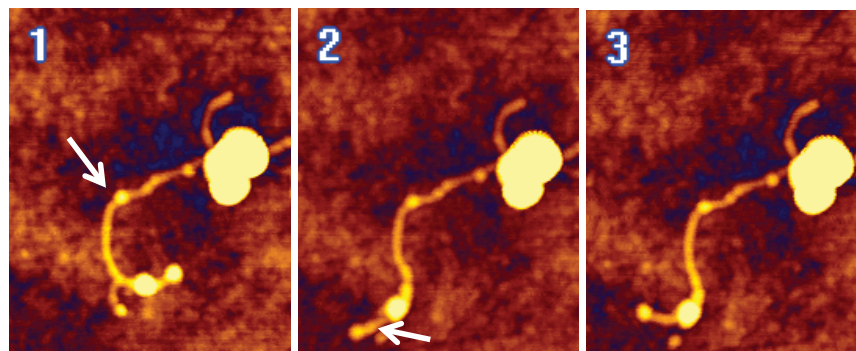
SPMs can be utilized not only for imaging but also for *local manipulation* and *patterning of surfaces*.

Examples: *Manipulation of single atoms* (see below), *nanolithography*, *nanopatterning* as well as mechanical manipulation of nano-objects (see next page).

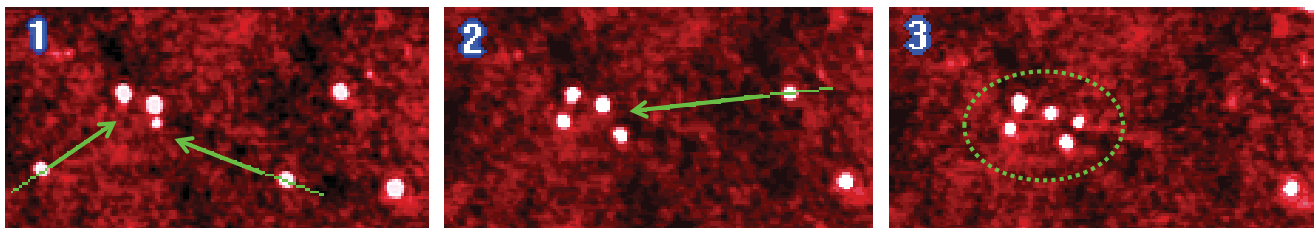
STM manipulation of iron atoms on a copper surface (Don Eigler et al., IBM)



Manipulation of Nano-objects using SPM



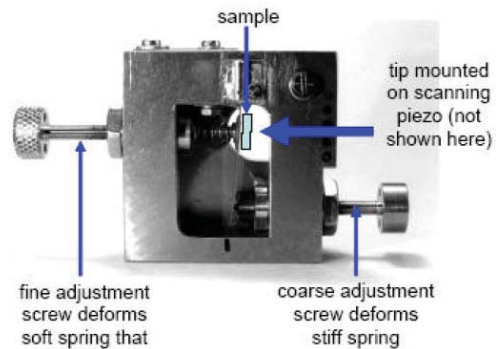
Nano wire manipulation on polymer film using contact mode with a force of 2.2nN.
Images taken in NC mode. Scan field 400 x 550 nm².



Manipulation of 5 nm CdSe quantum dots on glass in air. Imaging with NC mode, Manipulation in contact mode. 1.0 x 0.6 μm²

10.2.5 Miniaturization

- ❖ **Miniaturization** of SPM microscopes: Possible because resolution depends mainly on the tip radius and the tip-sample interaction (no need for bulky magnifying elements).
 - » SPMs can be incorporated easily into various measurement and preparation systems.



- ❖ **Breaking the “practical” law of microscopy** that for higher resolutions larger and more expensive instruments are needed (MeV, synchrotron radiation, etc.). In contrast, by SPM with **simple, small and cheap** table top instruments atomic resolution can be obtained.

10.3 Probe-Sample Interactions

Because a SPM does not have an “eye vision”, a probe-sample interaction is needed to induce a **“sensing” signal** by which the scanning of the tip over the sample surface can be controlled.

It can be compared with the “sensing feeling” of a finger tip that touches a surface while it is move over it.



Importance:

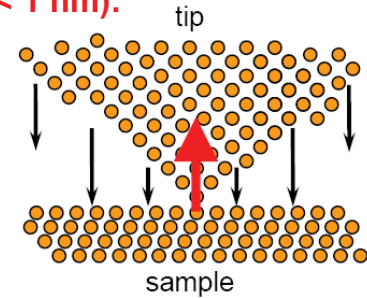
- ❖ The type of tip-sample interaction that is used for the scanning process determines the **type of SPM mode** (see above).
- ❖ In SPM, the **interaction strength** is used as a measure for the actual the tip-sample distance.
- ❖ During the scanning process this interaction strength is tried to be **kept constant**, meaning that the SPM tip follows the topography of the investigated sample surface.
- ❖ The tip-sample interaction determines to a large degree the **spatial resolution of SPM** in the **vertical** as well as **lateral direction**: The more **localized** and **short range** the interaction, the **higher the resolution** !

10.3.1 Mechanisms Contributing to the Tip-Sample Interaction

A wide range of different interaction mechanisms between tip and sample exist:

(A) Short-range interactions (contact & near contact, $s < 1$ nm):

- Short-range repulsive forces at $s < 1$ Å due to inner shell (Pauli exclusion) or ionic repulsion forces. Large forces but very short decay length (fraction of atom diameter).
- Short-range attractive forces: **Chemical bonding**, covalent due to wave function overlap, or metallic or ionic bonds. Range ~ 1 atomic unit: 0.5 Å for metallic adhesion, ~ 2 Å for covalent or molecular bonds.
- Overlap of the electronic wave functions of the tip and the sample atoms results in an electron transfer by tunneling that leads to a tunneling current that can be detected



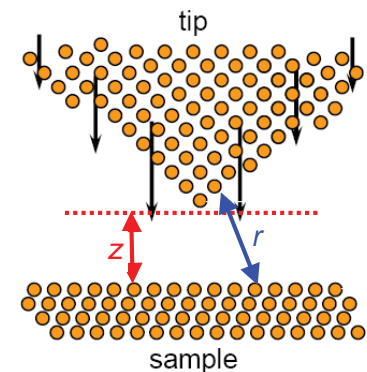
(B) Long-range interactions (non-contact, $s > 1$ nm):

- van der Waals interaction
- electrostatic, magnetic forces, ...

In liquids:

- hydrophobic / hydrophilic forces
- steric forces, solvation forces

⇒ Because the interactions have **very different ranges**, at a given distance typically one or few interactions dominate.



10.3.2 Other Tip-Sample Interactions

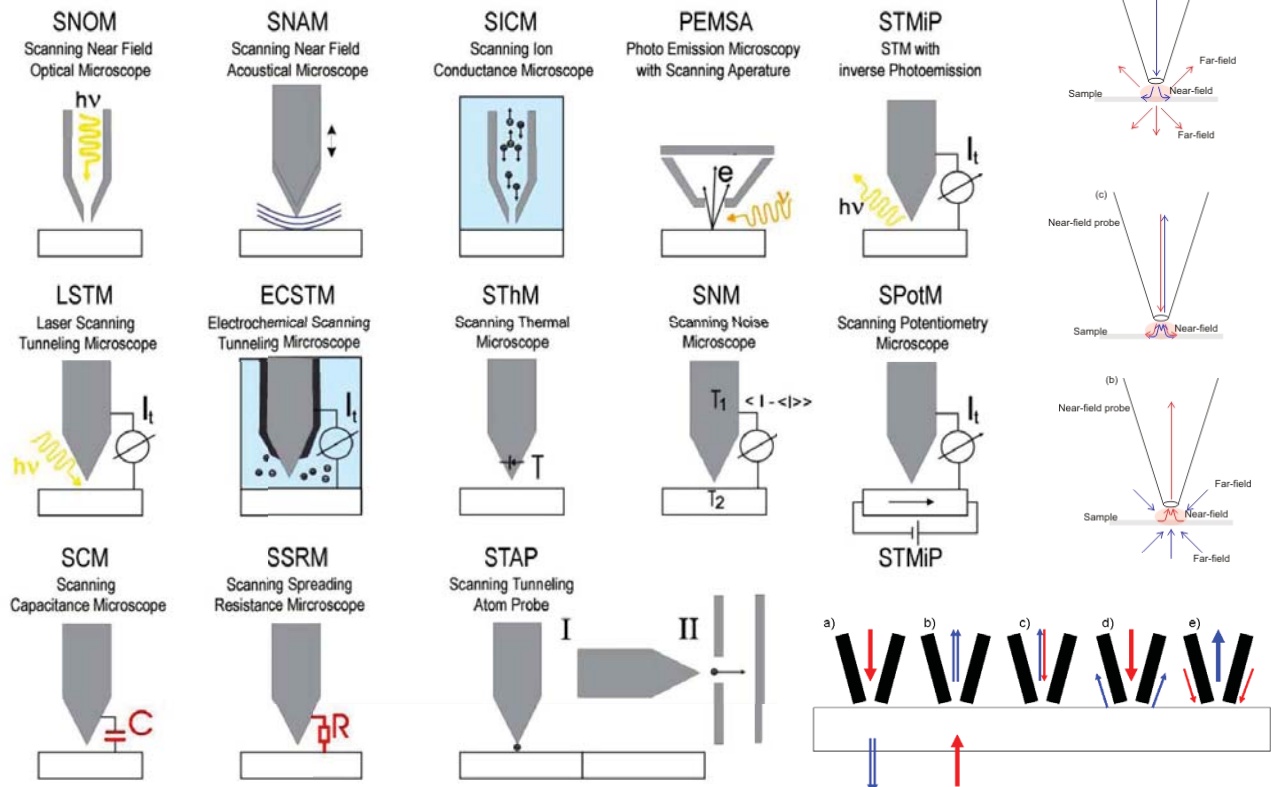
Apart from the forces and the tunneling current, these other types of interactions can also occur:

- ❖ Near field optical exchange: Coupling of electro-magnetic light to the sample by absorption, emission, polarization, photo-current, etc. .
- ❖ Electric interaction: e.g., capacitance between tip and sample, conductance, ballistic current transport, field emission, ion conduction in liquids, etc.
- ❖ Thermal exchange: Heat transport/exchange by temperature gradients/differences
- ❖ Near-field acoustic exchange: Excitation, propagation and damping of excited ultrasonic elastic waves induced by tip or sample modulation
- ❖ Mechanical exchange: Plastic deformations by nano indentation (hardness measurements, wear, tribology)

Note:

- ⇒ **Several interaction signals may be measured simultaneously** (see next section).
- ⇒ **Often, the interactions are significantly influenced by the environmental conditions.**

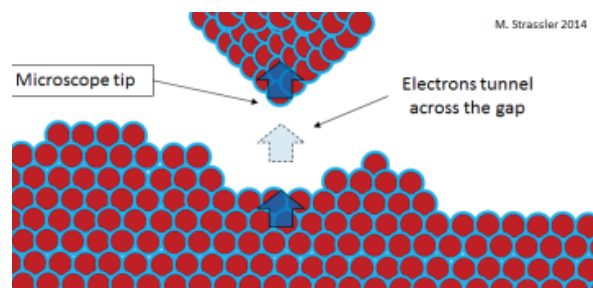
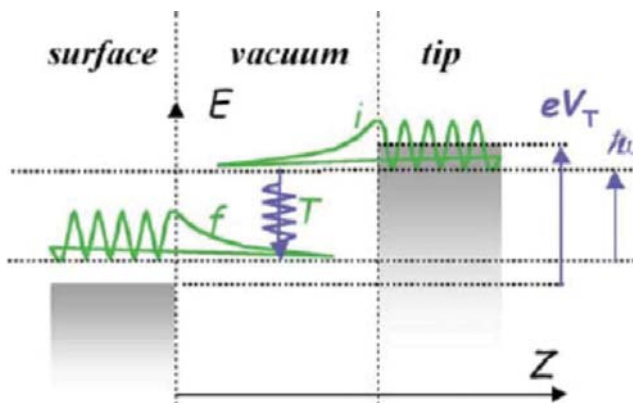
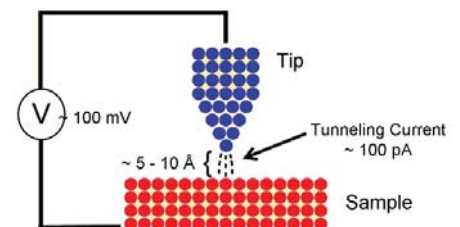
Measurement of additional interactions signals during the scanning process



10.4 The Tunnelling Current: STM

The tunneling current flowing between tip and sample is the most simplest way to measure the tip-sample interaction and it is a good measure of the actual tip-sample distance.

Due to the **tunneling effect**, this current flows when there is an **overlap of the wave functions** even if there is no real physical contact between tip and sample. As a result, a current flows when a voltage is applied and the tip-sample distance is very small ($\sim \text{\AA}$).



Outside of a solid, the electron **wave functions decay exponentially** with increasing distance from the surface, i.e., the probability of finding an electron outside of the solid of $\sim \text{\AA}$ per decade.

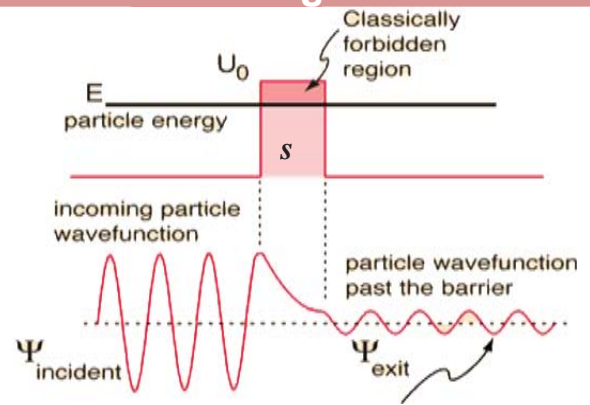
If two surfaces are brought very close to each other, the electron wave functions overlap and thus, a certain probability for tunneling of electrons through the vacuum from one solid to the other exists.

10.4.1 Quantum Mechanical Description of the Tunneling Process

The tunneling probability can be calculated by solving the time-independent Schrödinger equation for the electron wave function $\psi(x)$:

$$H\psi(x) = \left[-\frac{\hbar^2}{2m} \frac{d^2}{dx^2} + V(x) \right] \psi(x) = E\psi(x),$$

where H is the Hamiltonian, \hbar the Planck constant, m the mass, E the electron energy and $V(x)$ the potential barrier, which in the simplest case of a square shaped potential is simply given by the barrier height V_0 and width s .



Solution of the Schrödinger equation for the simple 1D square potential is obtained by assuming:

1. plane waves for the free electrons on the left and right hand side of the barrier and
2. an exponentially decaying wave function within the barrier.

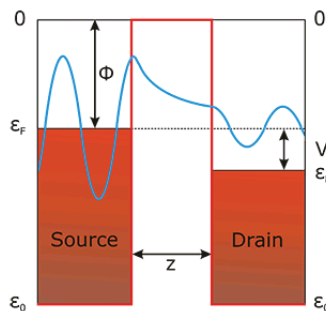
The wave functions and their derivatives must be continuous, i.e., equal at the boundaries, which leads to a set of equations that determine the amplitudes of the plane waves on each side of the barrier. The transmission probability is then equal to the squared ratio of amplitude of the plane wave on the right hand side to that of a plane wave incident on the left hand side. In the weak coupling limit (not too large overlap) this gives the tunneling or

Transmission probability vs barrier width s :
$$T = 2 \left(\frac{\kappa}{k^2 + \kappa^2} \right)^2 \cdot e^{-2\kappa s} \quad \text{with } \kappa = \sqrt{2m(V_0 - E)/\hbar^2}$$

where $V_0 - E$ is the barrier height given by the work function of the material and s the width of the barrier

⇒ The transmission probability **decreases exponentially** with increasing tip-sample distance s !!

Barrier height:



Work function $\phi_a = V_0 - E \approx 4\text{eV}$

Table 1.1. Typical values of work functions. After *Handbook of Chemistry and Physics*, 69th edition, CRC Press (1988).

Element	Al	Au	Cu	Ir	Ni	Pt	Si	W
ϕ (eV)	4.1	5.4	4.6	5.6	5.2	5.7	4.8	4.8

Damping coefficient: $\kappa = \sqrt{2m(V_0 - E)/\hbar^2} = 1.02 \text{ \AA}^{-1}$

Distance dependence: The transmission probability

T decreases very strongly with increasing s :

For $\phi_a = V_0 - E \sim 4\text{eV}$ » decay constant $\kappa = 1.02 \text{ \AA}^{-1}$

Thus, for $\Delta s = 1 \text{ \AA}$ » $\Delta T/T = e^{-2\kappa(s+\Delta s)}/e^{-2\kappa s} = e^{-2\kappa \Delta s} = \mathbf{1:7.4}$

» A change in tip-sample distance by $\Delta s = 1 \text{ \AA}$ results in ~ factor of 10 change of transmission probability and thus of the tunneling current !

» **Very high z resolution:** $\Delta z = 0.1 \text{ \AA} \rightarrow \Delta I_t/I_t = 20\% !$

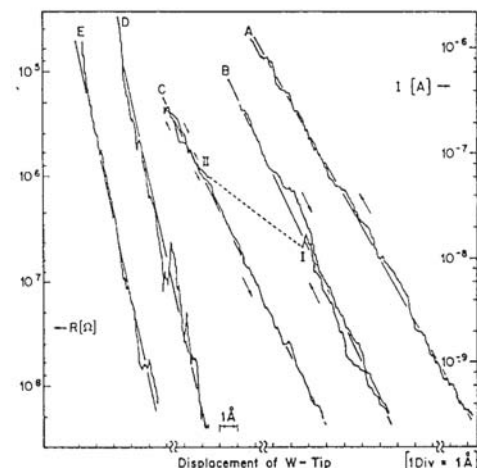


Fig. 1.6. Tunneling through a controllable vacuum gap. The exponential dependence $I \sim e^{-\kappa z}$ is observed over four orders of magnitude. On clean surfaces, an apparent barrier height of 3.5 eV was observed. (Reproduced from Binnig et al., 1982a, with permission.)

10.4.2 Consequences for the Lateral Resolution of STM

The **very high z resolution of STM** [$\Delta I/I_t = 20\%$ for $\Delta z = 0.1 \text{ \AA}$] results also in a **very high lateral resolution Δx** due to the **concentration of tunneling current at the apex of the STM tip** where the distance s is minimal.

Simple estimate for the lateral resolution of STM:

Lateral current distribution $I(x) \sim T(x)$ for a spherical tip with radius R : ($T = C \cdot e^{-\kappa \cdot s}$)

$$s(x) = s_0 + R(1 - \cos\varphi) \approx s_0 + x^2/2R$$

and

$$I(x) = I_0 \cdot \exp(-2\kappa x^2/2R)$$

Distance at which $I(x)$ has decreased to 1/10 of I_0 :

$$0.1 \cdot I_0 = I_0 \cdot \exp(-2\kappa x^2/2R) \gg x_{1/10} = (R \ln 0.1 / \kappa)^{1/2}$$

Example:

$R = 1000 \text{ \AA}$:	$x_{1/10} \approx 48 \text{ \AA}$
$R = 100 \text{ \AA}$:	$x_{1/10} \approx 15 \text{ \AA}$
$R = 10 \text{ \AA}$:	$x_{1/10} \approx 4.8 \text{ \AA}$
$R = 2 \text{ \AA}$:	$x_{1/10} \approx 2 \text{ \AA}$

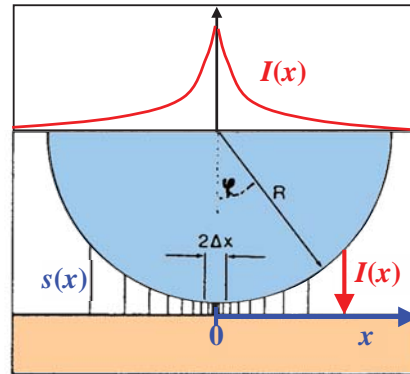


Fig. 1.7. Estimation of the lateral resolution in STM. In 1978, Binnig made an estimation of the possible lateral resolution of STM with a simple spherical-tip model. The tip end, with radius R , is very close to the sample surface. The tunneling current is concentrated in a small region around the origin, $x = 0$. With $r \approx 1000 \text{ \AA}$, the radius of the tunneling current column is approximately $\Delta x \approx 45 \text{ \AA}$. (After Quate, 1986.)

» Thus, a **single atom** at the end of the STM tip **carries ~90% of tunneling current** !

10.5 Force Interactions and Force Detection: AFM

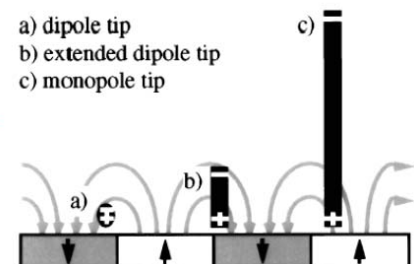
10.5.1 Microscopic and Macroscopic Forces

In **atomic force microscopy**, the **tip-sample force** is the primary signal for characterization of the tip-sample interaction as well as the tip-sample separation. It contains several different contributions:

- Repulsive contact forces:** Lenard Jones potential: $F \sim (\sigma/r)^n$, $n = 10 \dots 13$, $\sigma = \text{atom radii}$,
Born Mayer potential: $F \sim e^{-r/\sigma}$, $\sigma \sim 0.3 \text{ \AA}$ (metals).
- Contact adhesion** (Chemical bonding): Very short range (1-2Å). Bonding force between atoms: $\sim 1 \dots 10 \text{ nN}$
- Electrostatic forces** (\pm) between permanent point charges (insulators) or permanent dipoles:
charges: $F \sim -q^2/(4\pi\epsilon_0 r^2)$; dipoles: $F \sim -q^2/r^4$ (orientation dependent)
- Magnetostatic forces:** Dipole-dipole forces $F \sim -q^2/r^4$,

Depends strongly on the relative dipole orientation, and the **magnetic stray fields** of sample and the magnetization direction of the AFM tip

Attention:
the magnetic force is rather proportional to the stray field (and NOT to the derivative of the stray field as documented in many manuals of SPMs and publications !!!)



- Van der Waals forces** (Attractive)
= Dipole interaction due to non-permanent dipoles resulting from charge fluctuations in materials. Quantum mechanical origin. Strongly depends on the medium between the tip and sample. Can reverse the sign in liquids.
Range: 2-1000Å, between two atoms: $F(r) \sim -\alpha_1 \alpha_2 / r^7$, α : polarisability

- **Lateral frictional forces** during relative lateral tip motion, act against the direction of tip movement.
- **Capillary forces** due to meniscus of medium between tip and sample (surface tension),
In air due to water film on the surface

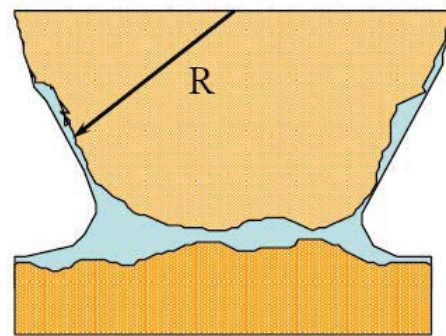
$$F_{\max} = 4 \pi R \gamma \cos(\Theta)$$

$$\gamma (\text{H}_2\text{O}) = 0.074 \text{ N/m}$$

$$R = 100 \text{ nm}$$

Contact angle for hydrophilic surfaces $\Theta \approx 0^\circ$

$$\Rightarrow F_{\max} = 90 \text{ nN}$$



- **Elastic and plastic deformation forces** for direct mechanical contact between the tip and sample.

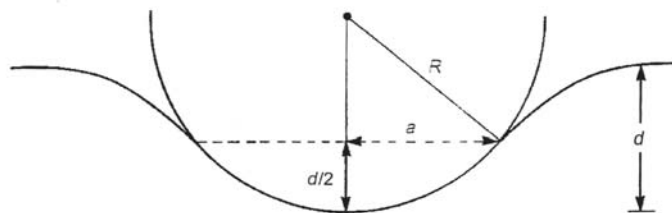


Figure 10.1. A sphere with radius R in contact with a flat surface. The radius of the contact area is a and the penetration depth is d .

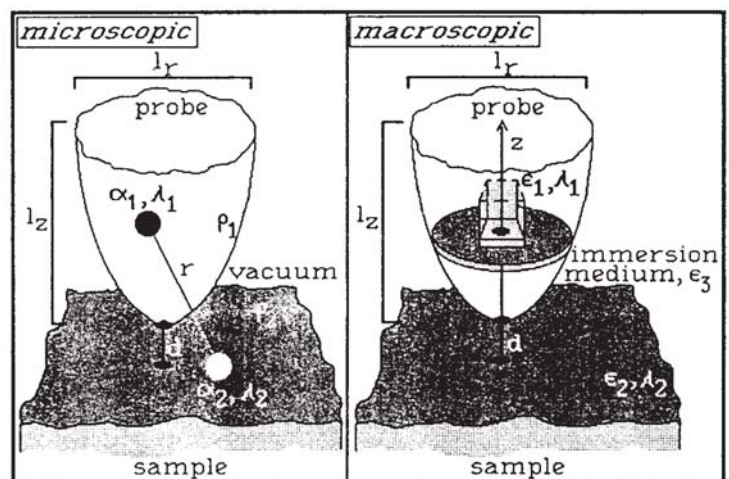
$$F = Kda = \frac{Ka^3}{R} = (K^2 R d^3)^{1/2}$$

Macroscopic Force between Tip and Sample

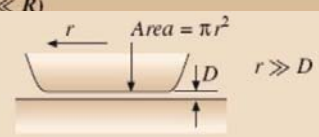
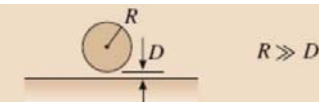
- ⇒ Summation over the contributions of all mass elements of the tip and sample,
- ⇒ important for long range interactions where

$$F \sim r^{-n} \quad n = 2 \dots 4$$

Example: Van der Waals force between a sphere of radius R and a planar surface at a separation z :



- (a) $z \ll R$: $F(z) = - (A_H R) / (6 z^2)$ with **A_H = Hamaker constant** $= \pi^2 C \rho_1 \rho_2$ (ρ = atom density) $\sim 1 \text{ eV}$
- (b) $z \gg R$: $F(z) = - (A_H R^3) / (3 z^4)$ C = Proportionality constant of VDW potential $U_{\text{vdw}}(r) = -C / r^n$

Geometry of bodies with surfaces D apart ($D \ll R$)		van der Waals interaction	
		Energy, E	Force, F
Two flat surfaces (per unit area)		$\frac{-A_H}{12\pi D^2}$	$\frac{-A_H}{6\pi D^3}$
Sphere or macromolecule of radius R near a flat surface		$\frac{-A_H R}{6D}$	$\frac{-A_H R}{6D^2}$

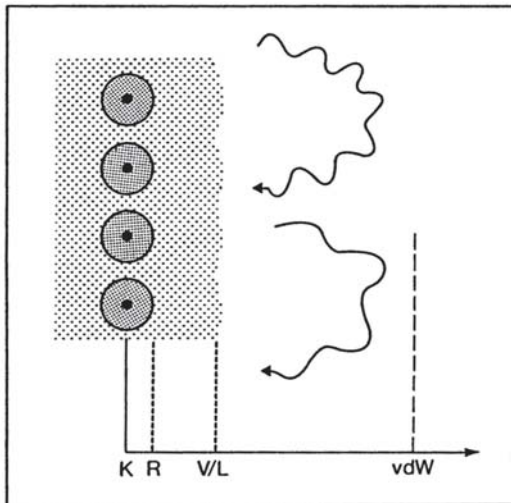
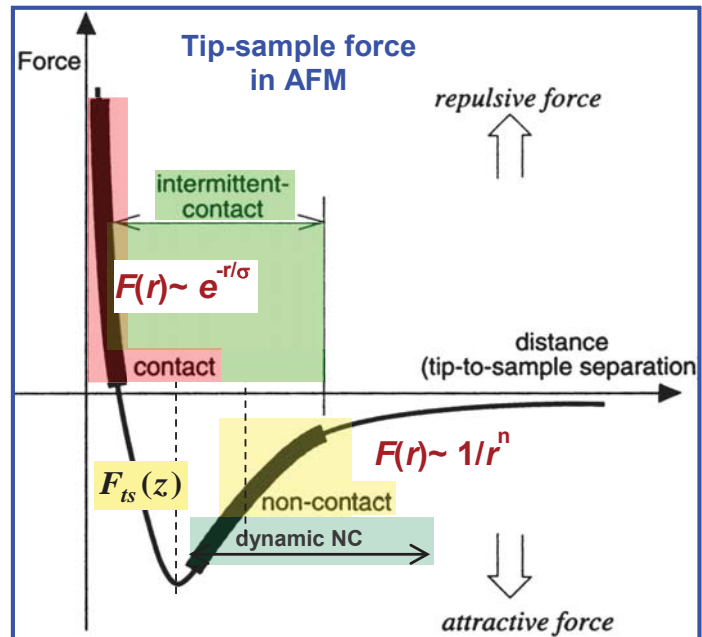


Abb. 3: Die drei Grenzen an der Oberfläche eines Festkörpers. K = Atomkerne; R = Rumpfelektronen; V/L = Valenz-/Leitungsbandelektronen; vdW = Reichweite der van der Waals-Kraft.



⇒ For a given tip sample separation often one force contribution dominates !

⇒ **Different regimes:** Contact, intermittent contact non-contact regime.

10.5.2 Force Sensors: Micromechanical Cantilevers

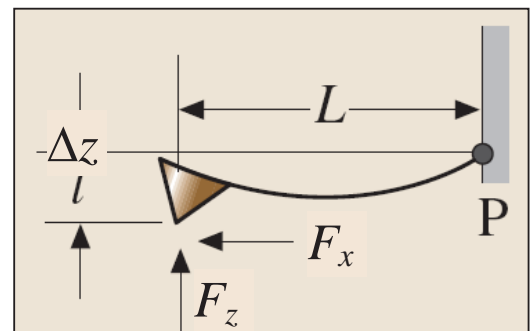
Generally, forces are measured using a **spring sensor**, in which case the force F_z acting on a spring leads to a length change or deflection dz of the spring.

In AFM, not a spiral spring but a **cantilever** spring is used due to the simpler fabrication.

The relation between the force acting on the cantilever end and cantilever deflections is given by the **Hook's law**:

$$F_z = k_{c,z} \cdot \Delta z \quad \text{with } k_{c,z} = \text{cantilever force constant}$$

⇒ Thus, the **measurement of vertical cantilever deflection Δz** yields magnitude of the vertical force acting between tip and sample surface.



Typical interatomic force constants are of the order of 10 N/m, depending on bonding type).

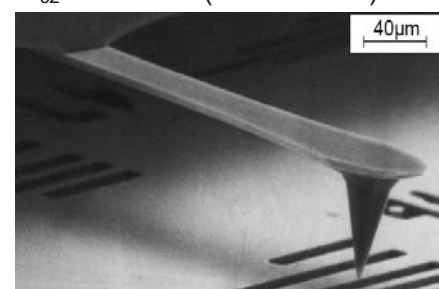
Typical cantilever force constants for contact mode AFM: $k_{c,z} = 0.01 - 10 \text{ N/m}$

Magnitude of deflection: For $\Delta F_z = 0.1 \text{ nN} \gg \Delta z = 10 \text{ \AA}$ for $k_{c,z} = 0.1 \text{ N/m}$ (in NC mode).

Basic considerations:

(a) Small k : Large deflection for small ΔF
 » **high sensitivity**, important for **soft samples**.
 But: High sensitivity to environmental noise.

(b) Large k : Smaller sensitivity but **higher stability**.
 (also higher resonance frequencies).



10.5.3 Cantilever Design

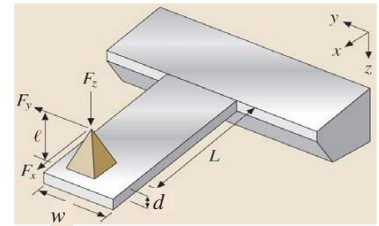
1. Spring constant in the range of 0.01 – 100 N/m:

The **force constant** k_{cz} of a cantilever is determined by its geometry, i.e., length L , thickness d and width w , as well as by the elastic constants (elastic modulus E) of the cantilever material.

For simple cantilever geometries with constant cantilever cross section, the force constant can be calculated analytically using elasticity theory

Rectangular beam of width w , length L , and thickness d , elasticity module E and a tip at a distance Δs from the end:

$$k_{cz} = E \cdot \frac{w \cdot d^3}{4 \cdot (L - \Delta s)^3}$$



⇒ By choice of the geometry the spring constant can be tuned arbitrarily over a wide range !

Common cantilever and tip materials:

Property	Young's Modulus (E) (GPa)	Density (ρ) (kg/m ³)	Microhardness (GPa)	Speed of sound ($\sqrt{E/\rho}$) (m/s)
Diamond	900–1,050	3,515	78.4–102	17,000
Si ₃ N ₄	310	3,180	19.6	9,900
Si	130–188	2,330	9–10	8,200
W	350	19,310	3.2	4,250
Ir	530	—	~ 3	5,300

Force Constant of Cantilevers with Different Cross-Sections

The influence of the cantilever shape is described by the **moment of inertia** $I = \int w(z) \cdot z^2 \cdot dz$ where $w(z)$ is the cross-sectional width of the cantilever at a distance z from the plane.

Verical Force Constanz k_{cz} :

Rectangular beam:

(width w and thickness d):

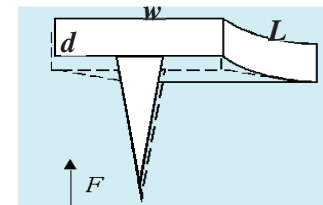
Cantilever with the tip at a distance Δs from the end:

$$I_{bar} = \frac{w \cdot d^3}{12}$$

$$k_{cz} = 3EI / L^3$$

$$k_{cz} = E \cdot \frac{w \cdot d^3}{4 \cdot L^3}$$

$$k_{cz} = E \cdot \frac{w \cdot d^3}{4 \cdot (L - \Delta s)^3}$$

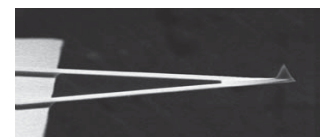


Circular rod:

(length l , diameter d):

$$I_{cylinder} = \frac{\pi \cdot r^4}{4}$$

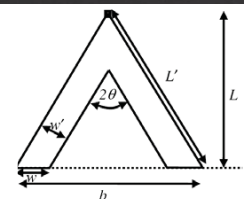
$$k_{cz} = E \cdot \frac{3 \cdot \pi \cdot d^3}{4 \cdot L^3}$$



V-shaped cantilever:

(length L , thickness d , leg width w , half angle θ , leg distance at base b)

$$k_{cz} = \frac{E \cdot w \cdot d^3}{2 \cdot L^3} \cos \theta \left[1 + \frac{4w^3}{b^3} (3 \cos \theta - 2) \right]^{-1}$$

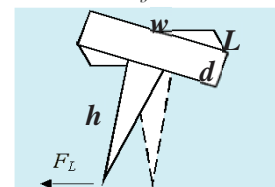


Lateral Force Constant $k_{lateral}$

(Rectangular beam, tip height h):

(G = shear modulus)

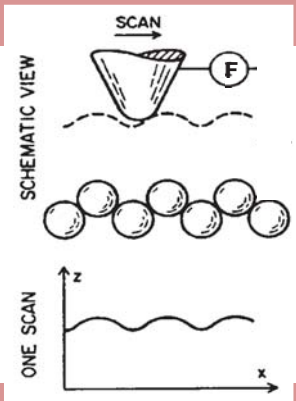
$$k_{lateral} = G \cdot \frac{w \cdot d^3}{L \cdot (h + d/2)^2}$$



2. Dynamic response of the cantilever

During the scanning process, the cantilever and tip should be able to **follow the rapidly changing surface topography** of the sample (=fast dynamical response) and the transient acceleration forces acting on the tip should be kept as small as possible:

- ⇒ The **inertial cantilever mass size should be very small !**
This means small cantilever size, i.e., **cantilever miniaturization**.



3. Suppression of cantilever excitation

The cantilever should be immune against **internal excitations** arising from the scanning process as well as against **external excitations** due to mechanical vibrations, acoustic & thermal noise, ..).

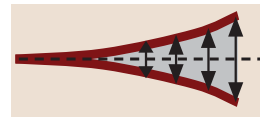
Example:

- 2 μm scan of a 10 nm periodic structure with 5 Hz scan rate = 1 kHz vertical excitation of the cantilever
- 30 nm scan of a 3 Å atomic lattice with 10 Hz scan rate = 1 kHz vertical excitation of the cantilever
- Alternative: Low scan rates such as 1 Hz/line, 500 lines / image = 8 min / image

Generally, the **reaction of a cantilever** is similar to that of a **damped harmonic oscillator**.

This means that the cantilever reacts strongly mainly to excitations with a frequency close to the Eigen-resonance frequency of the cantilever, i.e., the cantilever response speed is **limited by the lowest cantilever resonance frequency** due to simple bending oscillation.

» This **resonance frequency** $\omega_{0,\text{res}}$ should be at **above 10 kHz** to prevent strong cantilever excitations !



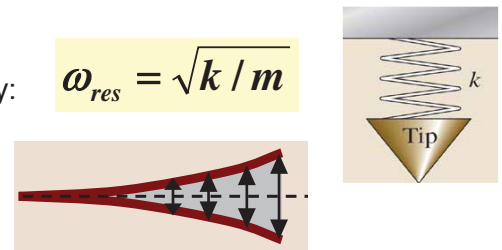
4. Resonance Frequency ω_{res} of the Cantilever

The **fundamental resonance frequency** a **simple spring-type harmonic oscillator** (mass load attached to a spring) is given by:

$$\omega_{\text{res}} = \sqrt{k / m}$$

For a **cantilever** the situation is somewhat different because the cantilever **mass is distributed along the cantilever beam**.

Thus, different cantilever parts oscillate with different amplitude and velocity.



Rayleigh solution: = Equating the maximum kinetic energy and maximum strain energy of the cantilever, where: $z(x,t) = z_0(x^4 - 4x^3L^2 + 6x^2L^2) / L^4 \cdot \sin(\omega t)$ for the free ended cantilever.

By integration from $x = 0$ to L , one obtains: $E_{\text{strain}} = 1/2 \cdot (1.6 \cdot k_c) z_0^2$ and $E_{\text{kin}} = 1/2 \cdot (0.256 \cdot m_c) \cdot \omega^2 z_0^2$

Lowest frequency mode:
(vertical bending mode)

$$\omega_{\text{res}} = \sqrt{\frac{k_c}{0.24 \cdot m_c}}$$

or with additional tip mass m_{tip} :

$$\omega_{\text{res}} = \sqrt{\frac{k_c}{0.24 \cdot m_c + m_{\text{tip}}}}$$

Higher order modes:

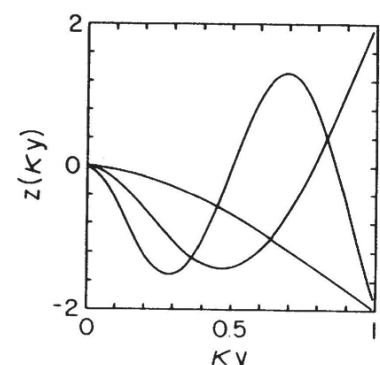
$$\omega_n = \frac{\kappa_n^2}{L^2} \sqrt{\frac{E \cdot I}{\rho \cdot A}}$$

with $\kappa_n = 1.875, 4.694, 7.855, 10.996, \dots$ and

$m_c = \rho \cdot V = \rho \cdot A \cdot L$ and $k = 3EI / L^3 = E \cdot w \cdot d^3 / 4L^3$

V-shaped cantilever:

$$\omega_{\text{res}} \approx \sqrt{\frac{k_c}{0.163 \cdot m_c + m_{\text{tip}}}}$$



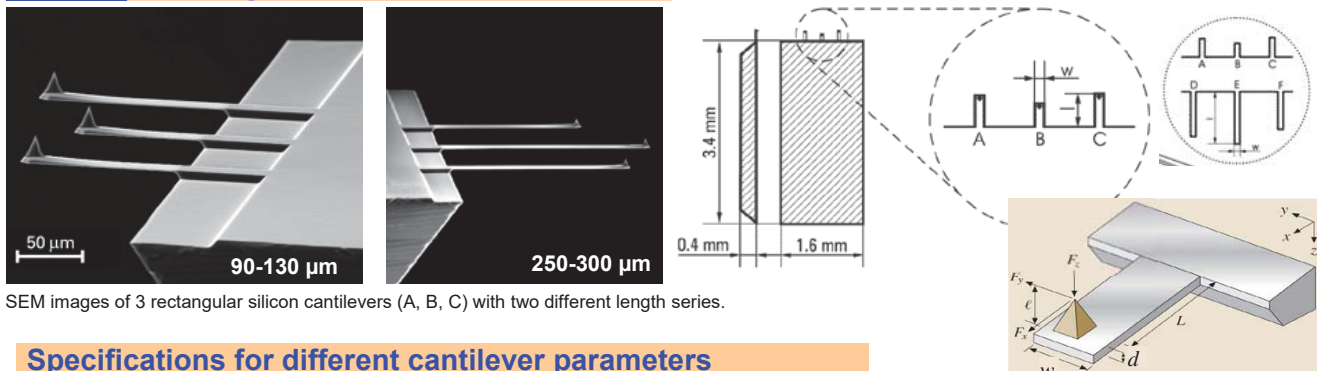
The first three modes of vibration of a lever.
X / 26

From the equations above it follows that for a given k -value, defined by the geometry and shape of the beam, a **high resonance frequency can be achieved by reducing the cantilever mass**.

This means **miniaturization of the cantilever beams** to achieve a high resonance frequency !

⇒ If w and the d/L ratio is fixed, then k is constant and ω_{res} increases if L is made very small.

Example: Rectangular bar-shaped cantilevers made of silicon



SEM images of 3 rectangular silicon cantilevers (A, B, C) with two different length series.

Specifications for different cantilever parameters

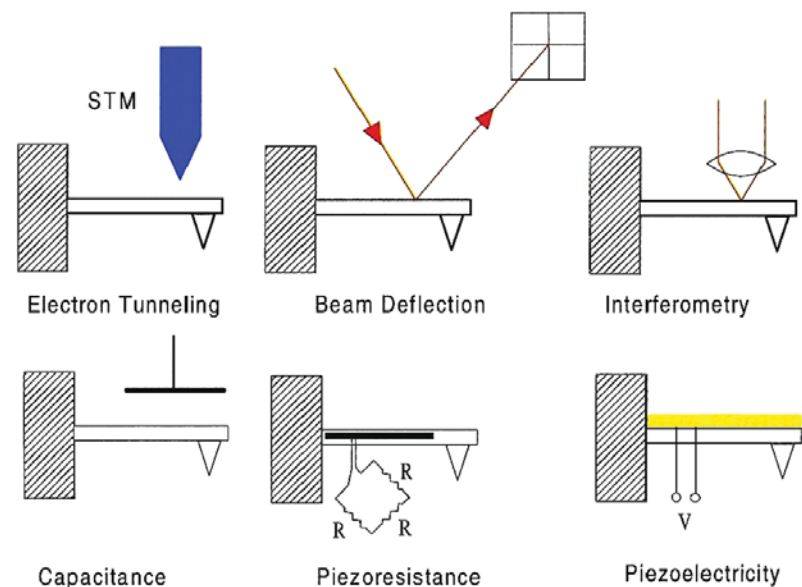
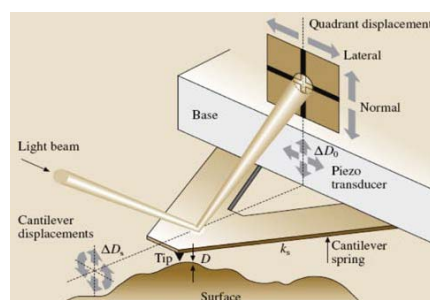
Cantilever Type	Length, $L \pm 5 \mu\text{m}$	Width, $w \pm 3 \mu\text{m}$	Thickness, $d \mu\text{m}$	Resonant Frequency, kHz	Force Constant, N/m
A	$110 \pm 5\%$	$35 \pm 8\%$	$2.0 \pm 10\%$	$210 \pm 20\%$	$7.5 \pm 30\%$
B	90	35	2.0	315	14.0
C	130	35	2.0	150	4.5
A	110	35	1.0	105	0.95
B	90	35	1.0	155	1.75
C	130	35	1.0	75	0.60

10.5.4 Measurement of the Cantilever Beam Deflection

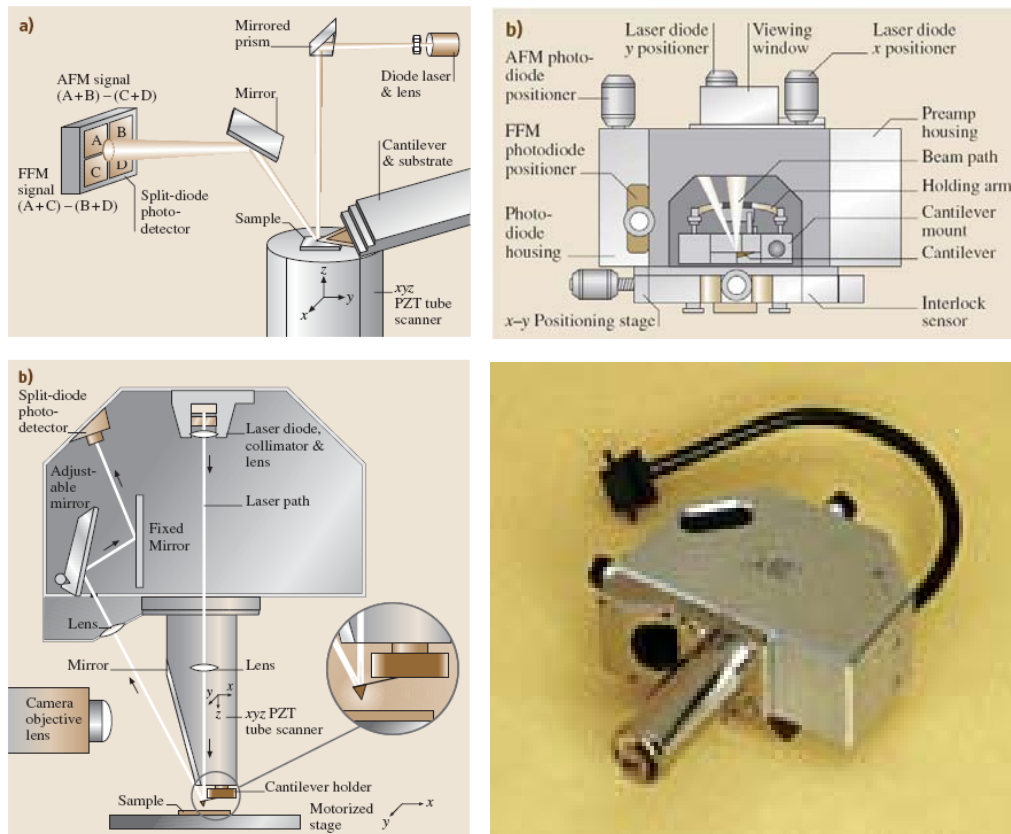
Requirements:

Sub-Å sensitivity
for vertical cantilever deflection.

Basic approaches:



- **Electron Tunneling:** Original concept, potentially sensitive, practically problematic.
- **Laser beam Deflection:** Most widely used, robust, high sensitivity, force calibration required.
- **Interferometry:** Best sensitivity, quantitative, uses limited space, complicated.
- **Capacitance:** Sensor can be micro fabricated, strong force from sensor, limited sensitivity.
- **Piezoresistance:** Ideal for microfabrication & integration, limited sensitivity, heating of cantilever.
- **Piezoelectric:** Quartz tuning forks, Good for atomic resolution due to high sensitivity in dynamic mode.



10.6 Comparison: Atomic Resolution in AFM / STM

Atomic resolution in AFM is *much more difficult* to achieve than in STM because the **local interaction** force between the final atom at the end of the tip and the surface atoms of the sample **is superimposed** by the large contribution of **long-range** van der Waals and other forces.

Therefore, in AFM **atomic resolution** can be achieved only by scanning the tip very close to the surface such that the tip force is able to sense the temporary local bonding due to overlap of the atomic orbitals of the tip and sample atoms and by using *very high sensitivity AC modulation force measurement schemes* (see Sect. 10.10 below).

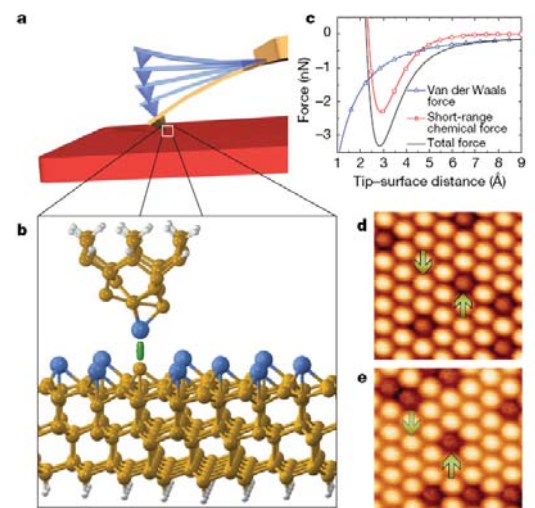
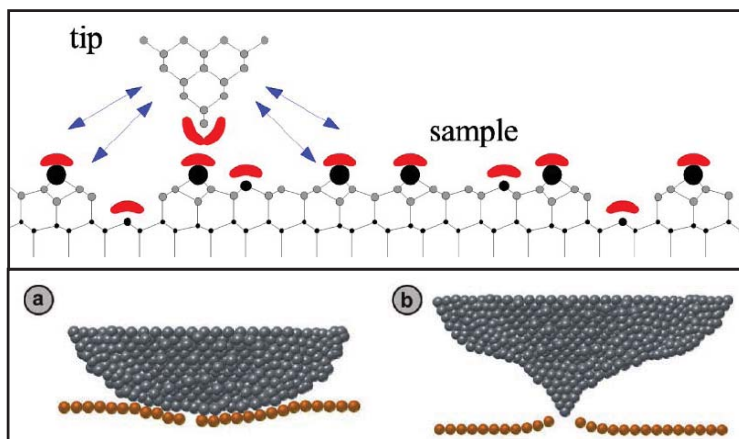
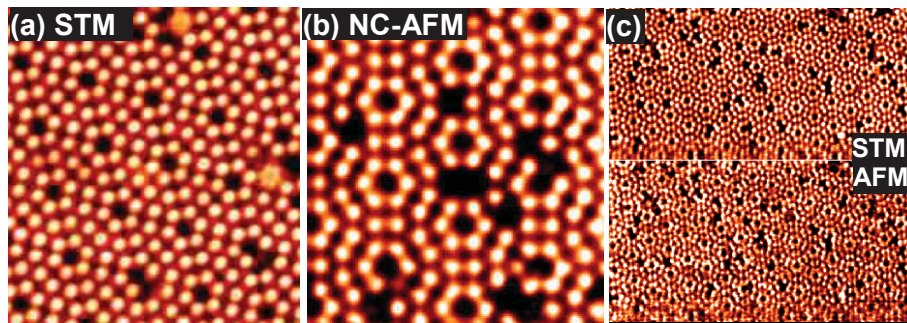


Figure 1 | Dynamic force microscopy with atomic resolution. Schematic illustration of AFM operation in dynamic mode (a), and of the onset of the chemical bonding between the outermost tip atom and a surface atom (highlighted by the green stick) that gives rise to the atomic contrast^{14,15} (b). However, the tip experiences not only the short-range force associated with this chemical interaction, but also long-range force contributions that arise from van der Waals and electrostatic interactions between tip and surface (though the effect of the latter is usually minimized through appropriate choice of the experimental set-up). c, Curves obtained with analytical expressions for the van der Waals force, the short-range chemical interaction force, and the total force to illustrate their dependence on the absolute tip-surface distance. d–e, Dynamic force microscopy topographic images of a single-atomic layer of Sn (d) and Pb (e) grown, respectively, over a Si(111) substrate. At these surfaces, a small concentration of substitutional

Sugimoto et al., *Nature* **446**, 64 (2007).

The first **true atomic resolution by AFM** was shown for Si (111) by Giessibl et al. (Science 1996)



Example: Atomic Resolution of Si(111) 7 x 7 in UHV

- (a) STM: $U = 2 \text{ V}$, $I = 2.0 \text{ nA}$,
- (b) Non-Contact Mode AFM,
- (c) Multi-mode operation: Simultaneous measurement of the topography in STM mode using a conductive cantilever, and of the atomic scale variation of the force, i.e. cantilever deflection.

Atomic resolution of pentacene molecules on Cu(111)

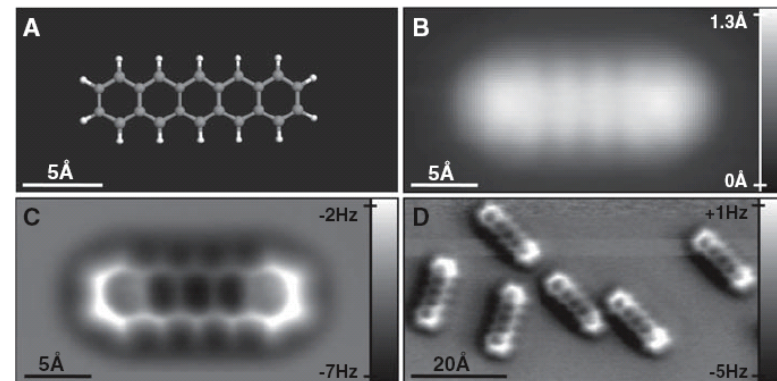


Fig. 1. STM and AFM imaging of pentacene on Cu(111). (A) Ball-and-stick model of the pentacene molecule. (B) Constant-current STM and (C and D) constant-height AFM images of pentacene acquired

L. Gross et al., *Science* **325**, 1110 (2009).

Sugimoto et al., *Nature* **446**, 64 (2007)

Atom identification of Pb,Sn on Si (111)

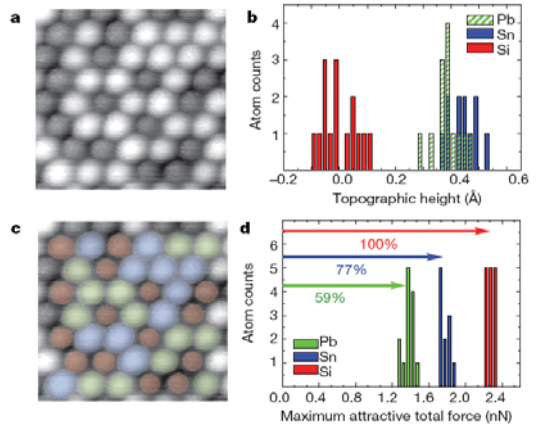


Figure 3 | Single-atom chemical identification. a, Topographic image of a surface alloy composed by Si, Sn and Pb atoms blended in equal proportions on a Si(111) substrate. b, Height distribution of the atoms in a, showing that Pb and Sn atoms with few nearest-neighbouring Si atoms appear indistinguishable in topography. c, Local chemical composition of the image in a. Blue, green, and red atoms correspond to Sn, Pb and Si, respectively.

10.7 Piezo Scanners

For controlled movement of the SPM tip over the sample surface a **highly precise 3D scanner** is required that allows to scan the tip over the sample surface with a **sub-nm resolution**.

Technical requirements:

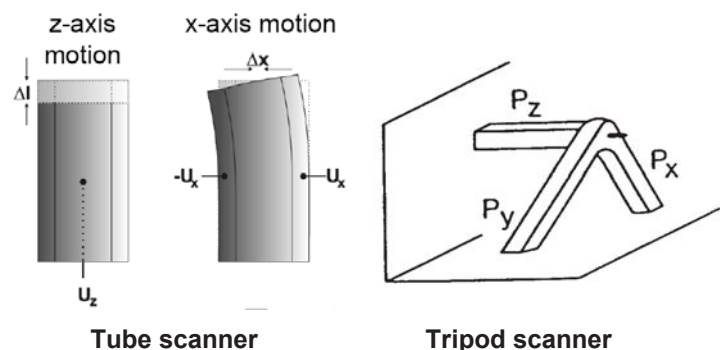
- 3D motion and positioning in **all three directions of space**
- **Control of the tip-sample separation** to better than $\Delta z < 0.1 \text{ \AA}$,
- Lateral scanning over a **sufficiently large scan range** $< \mu\text{m}$ with a precision $\Delta x < 1 \text{ \AA}$,
- High **linearity** and **reproducibility** of tip positioning and motion,
- **Small thermal drifts**, immune against mechanical and acoustic vibrations.

Practical realization: Piezo Scanners

SPM scanners are usually made using **piezoelectric elements**, made from **piezo-electric materials**, that change their length when a voltage is applied to them.

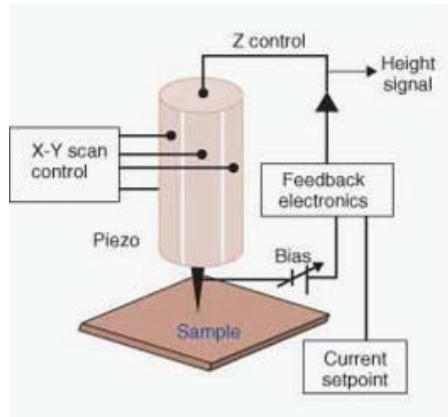
The expansion of piezoelectric elements is determined by the applied voltage.

Therefore, **arbitrarily small displacements** $\sim \text{\AA}$ can be easily realized and the stability and precision is mainly determined by the stability of the voltage source.



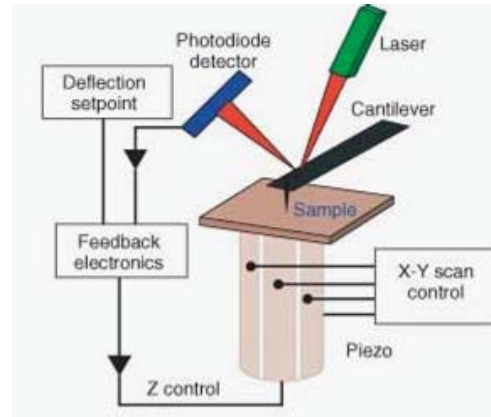
Typical designs are tube scanners, tripod scanners or flexure scanners.

(a) Tip-scanning systems



Most common for STM

(b) Sample scanning systems



More common for AFM

Advantages:

- » **Low inertial mass**, high resonance frequency.
- » Faster scanning.
- » **No limitation for sample size**.
- » Free sample access, e.g., for heating, cooling etc..

Disadvantages:

- » Moving tip makes optical measurement more difficult to implement

Other combinations: (x,y) sample scanning, z-movement of tip, etc. ...

Advantages:

- » **No lateral tip movement**; more easy implementation of optical detection

Disadvantages:

- » Higher inertial mass, slower scanning.
- » Limited sample size and weight.

10.7.1 The Piezoelectric Effect

In general: **Piezoelectric effect =**

Electric voltage or field at an insulator \Leftrightarrow Mechanical contraction or expansion

Discovered by Pierre and Jacques Curie (1880) by observation of an electric voltage at the side electrodes of a quartz crystal that is mechanically deformed under applied external stresses.

Lippman (1881): Theoretical prediction of the **inverse piezoelectric effect**, Experimental confirmation by the Curie brothers in 1882.

Origin: Relative displacement of the **positive** and **negative crystal lattice elements** against each other due to an applied external stress. This results in an electric polarization of the crystal.

Inverse effect: Applied electric field causes an ion displacement and thus expansion of the crystal.

Piezoelectricity occurs:

- ❖ **all anisotropic crystals**, i.e., in crystals without inversion center (i.e., in 20 of 32 crystal classes),
- ❖ only **insulators** are suited because for conductors the internal is always field free.
- ❖ The effect is usually very small except in **ferroelectrics**, i.e., in material which exhibit a spontaneous electrical polarization even without applied external fields.

Examples for strong piezo materials:

Quartz (» Quartz clocks, radiation sources, frequency standards, etc.)
BaTiO₃, PbTiO₃, PbZrO₃ (» ultra sonic generators and receivers, actuators).

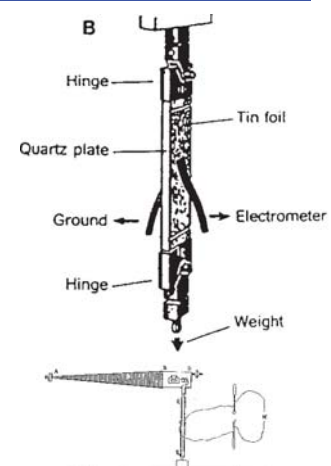


Fig. 9.2 The inverse piezoelectric effect. A thin and long quartz plate (QZ) is clamped between two tin foils. By applying a voltage to the tin foils, the quartz plate elongates or contracts according to the polarity of the applied voltage. To measure the very small displacement, Curie (1882) used a lever (L) with a small piece of glass attached to it. The displacement of the glass is then measured with an optical microscope. (after Curie, 1882c)

10.7.2 Displacement for a Piezo Plate due to Applied Voltage

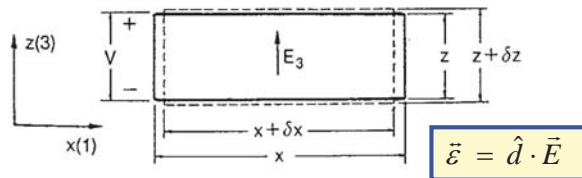


Fig. 9.3. Definition of piezoelectric coefficients. A rectangular piece of piezoelectric material, with a voltage V applied across its thickness, causes a strain in the x as well as the z directions. A piezoelectric coefficient is defined as the ratio of a component of the strain with respect to a component of the electrical field intensity.

Deformation (strain) induced by applied voltage U :

» Electric field E along z : $E_z = U/z$ or $= U/d$

$$\epsilon_{zz} = \Delta z / z = d_{zz} \cdot E_z \quad (\text{deformation in } z \text{ direction})$$

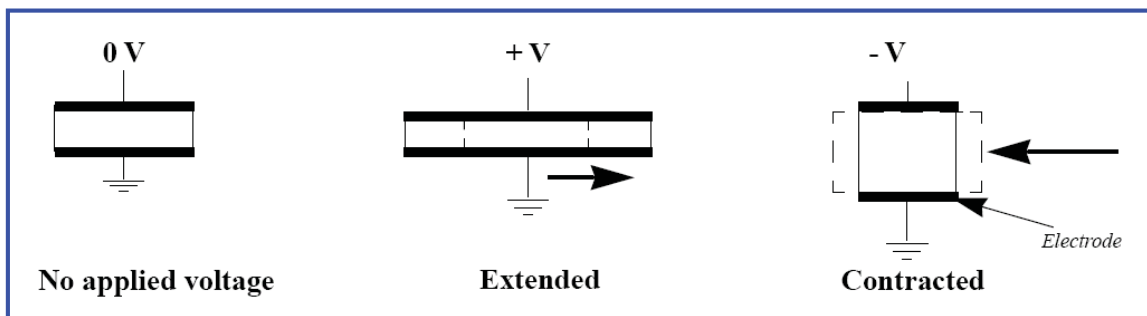
described by piezo modulus: $d_{zz} = \epsilon_{zz} / E_z$

» Simultaneous length change in x -direction:

$$\epsilon_{xx} = \Delta x / x = d_{xz} \cdot E_z \quad (\text{strain in } x \text{ direction})$$

described by piezo modulus: $d_{xz} = \epsilon_{xz} / E_z$

Dimension of piezo modules: d_{ij} [m/V] or [Å/V], Order of magnitude: $< \text{Å} / \text{V}$



Length Change of Plate with Electrodes on the Side Faces

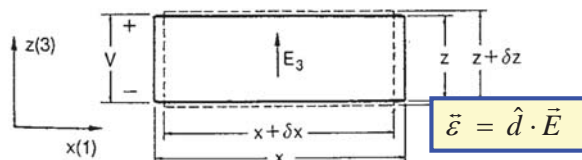


Fig. 9.3. Definition of piezoelectric coefficients. A rectangular piece of piezoelectric material, with a voltage V applied across its thickness, causes a strain in the x as well as the z directions. A piezoelectric coefficient is defined as the ratio of a component of the strain with respect to a component of the electrical field intensity.

The electric field E $E_z = U/z$ or $= U/d$ produces the deformations

$$\epsilon_{zz} = \Delta z / z = d_{zz} \cdot E_z \quad (\text{in } z \text{ direction})$$

and:

$$\epsilon_{xx} = \Delta x / x = d_{xz} \cdot E_z \quad (\text{in } x \text{ direction})$$

using piezo moduli d_{xz} and d_{zz} (units: $\sim \text{Å} / \text{V}$)

Resulting length change of piezo plate in x and z – direction perpendicular and parallel to E

$$\Delta x = x \cdot \epsilon_{xz} = x \cdot d_{xz} \cdot E_z = x \cdot d_{xz} \cdot U / z \Rightarrow \Delta x = d_{xz} \cdot U \cdot x / z$$

$$\Delta z = z \cdot \epsilon_{zz} = z \cdot d_{zz} \cdot E_z = z \cdot d_{zz} \cdot U / z \Rightarrow \Delta z = d_{zz} \cdot U$$

- » **Length change** in all directions **is linear in U !!** (first order approximation)
- » **Change Δz** parallel to the field is **independent of plate dimensions** ($\sim \text{Å} / \text{Volt}$).
- » **Change Δx** perpendicular can be **drastically amplified** by increasing the x / z ratio !
- » **Maximum** extension is limited by electrical **depolarization** and **break through fields**.

10.7.3 Tube Scanner

(invented by Binning and Smith, 1986)

= Piezo tube with **inner electrode** and **segmented 4 outer electrode**

- » Simplest design with high mechanical stability.
- » Used in most SPM instruments.

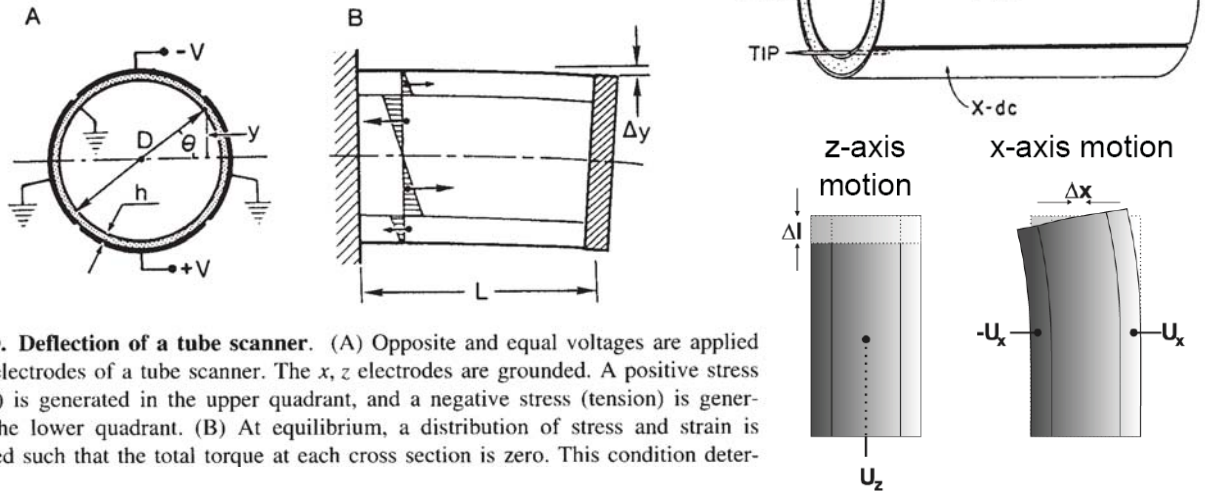


Fig. 9.10. Deflection of a tube scanner. (A) Opposite and equal voltages are applied to the y electrodes of a tube scanner. The x, z electrodes are grounded. A positive stress (pressure) is generated in the upper quadrant, and a negative stress (tension) is generated in the lower quadrant. (B) At equilibrium, a distribution of stress and strain is established such that the total torque at each cross section is zero. This condition deter-

z-displacement: Determined by voltage ΔU_z between inner / outer electrodes (~ same as for simple 2D plate)

$$\Delta z = d_{31} \cdot (L / h) \cdot \Delta U_z \quad L: \text{length}, h: \text{wall thickness}$$

Piezo constant:

$$K_{pz} = (\Delta z / \Delta U_z) = d_{31} \cdot (L / h)$$

Example: $K_{pz} = 80 \text{ Å/Volt}$, $\Delta z_{\max} \approx 3.2 \text{ μm}$

for $d_{31} = 2 \text{ Å/V}$, $L = 20$, $h = 0.5$, $D = 5 \text{ mm}$, $U = \pm 200 \text{ V}$

x,y displacement (due to anti-symmetrically driven electrodes)

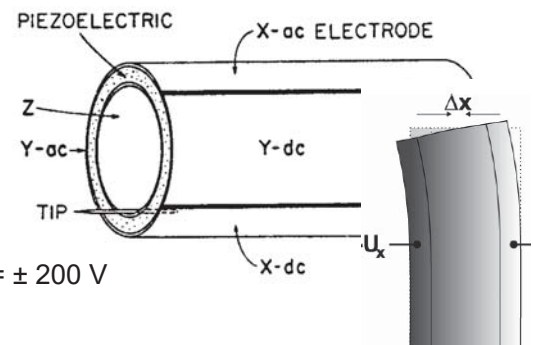
Opposite voltage is applied to opposite electrodes: $\Delta U_x = U_x^+ - U_x^-$

» x-displacement:
$$\Delta x = 2^{3/2} \cdot d_{31} \cdot (L^2 / D h) \cdot \Delta U_x$$

Piezo constant:
$$K_{px} = (\Delta x / \Delta U_x) = 2^{2/3} \cdot d_{31} \cdot (L^2 / D h)$$

Example: $d_{31} = 2 \text{ Å/V}$, $L = 20 \text{ mm}$, $h = 0.5 \text{ mm}$, $D = 5 \text{ mm}$, $U = \pm 200 \text{ V}$

» $K_{px} = 500 \text{ Å/Volt}$ » $\Delta x_{\max} \approx 20 \text{ μm}$
 » $K_{pz} = 80 \text{ Å/Volt}$ » $\Delta z_{\max} \approx 3.2 \text{ μm}$



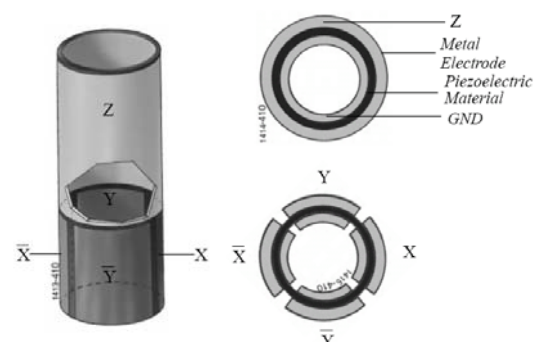
Alternative design

Features of Piezo tubes:

- Large displacements in x,y + precise movement in z direction,
- z-displacement is ~ perpendicular to x,y displacements,
- Center electrode is usually grounded.

Advantages of tube scanners:

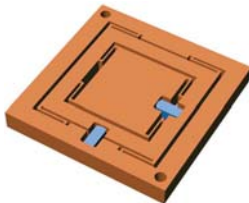
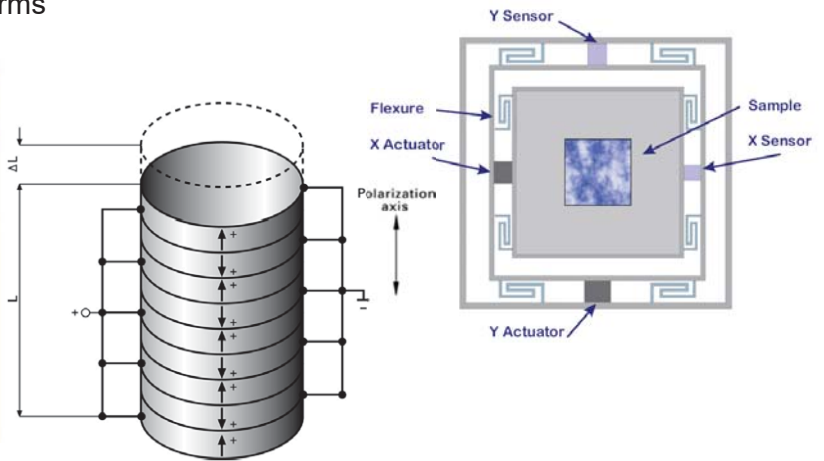
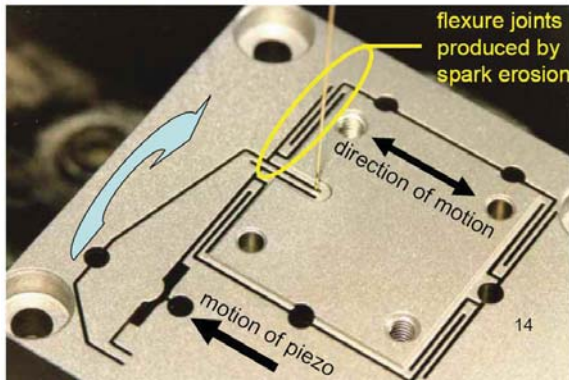
- Compact and simple design.
- Large x,y scan ranges possible with high vertical resolution.
- Good linearity for small scan range.
- High resonance frequency due to mechanical stability and low mass.



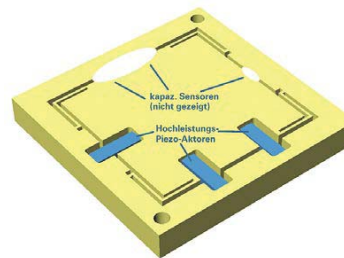
10.7.4 Flexure Scanner (x,y)

= Combination of piezo stacks and flexible arms

piezo flexure nanopositioners



$$\Delta z = N \cdot d_{zz} \cdot U = N \cdot 3\text{-}5 \text{ \AA/V} \cdot U$$



Advantages:

- Decoupling of x-y and of z motions,
- Planar 2D scanning in the x-y direction,
- Decoupled extra piezo tube for z-movement.

10.8 Imaging Strategies and Scan Modes

The imaging or scanning process of an SPM can be compared to a **blind exploration** of an object or environment by a probe stick (similar as a blind person with his stick) without having any vision or pre-knowledge on the topography of the sample.

Scan strategies: To solve this problem, one has to devise an efficient way on **how to scan the objects** without any prior knowledge about their structure and morphology. The goal is to explore the topography without damaging the probe tip or the sample, i.e., by avoiding too strong contact that would destroy the tip.



⇒ The only **feedback** sensing signal available this exploration process is the measurement of the strength of the tip-sample interaction. Due to the strong non-linearity of the tip-sample interaction, it is, however, only an indirect measure of the actual tip-sample distance.

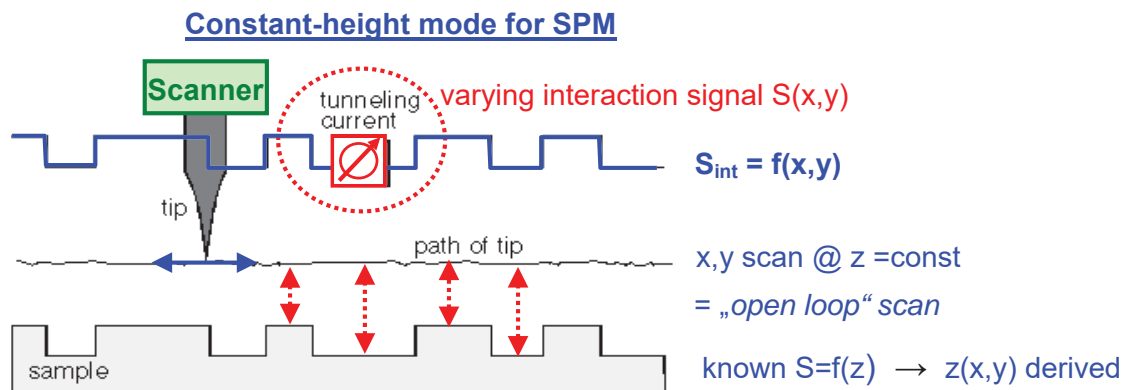
⇒ **Two fundamental scan and imaging approaches** can be used, called **constant height** or **constant interaction** scan mode.

In addition, further scan modes exist such as **hybrid or multi-pass scan modes** in which usually different types of interaction signals are recorded simultaneously or sequentially, which allows to obtain additional, non-topographic information such as electrical, magnetic or other properties.

10.8.1 Constant Height Mode

= Scanning at a constant z-level above the average sample height

The tip-sample interaction strength is simply measured $S_{\text{int}} = f(x,y)$ versus lateral tip position at $z = \text{constant}$.



(i) **Homogenous sample:** If the dependence of $I_{\text{int}}(z)$ is known, then the interaction image can be converted into a topographic image by calculating $z(I_{\text{int}}(x,y))$.

(ii) **Smooth & atomically flat sample surface:** Image corresponds to the **local variation of the microscopic sample properties** such as local work function, electronic density of states, electrical, optical, elastic, ...

» **Advantage:** No feed-back loop needed for regulating tip-sample distance: » lower noise / higher resolution.

» **Disadvantage:** Works only for smooth samples, not straightforward image interpretation.

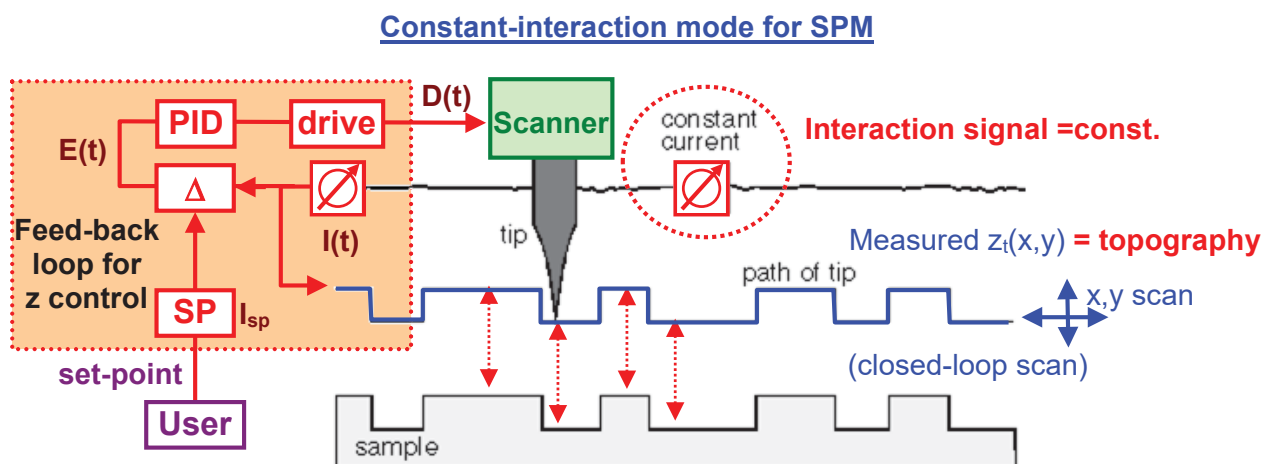
10.8.2 Constant Interaction Mode

= Constant current, constant force, etc. ...

During lateral scanning of the tip over the sample surface, a **feedback loop** constantly readjusts the z-position of the tip in the vertical direction such that the **tip-sample interaction signal** is kept **constant**.

» The path of the tip $z_{\text{tip}} = f(x,y)$ thus follows exactly the **topography** of the sample !

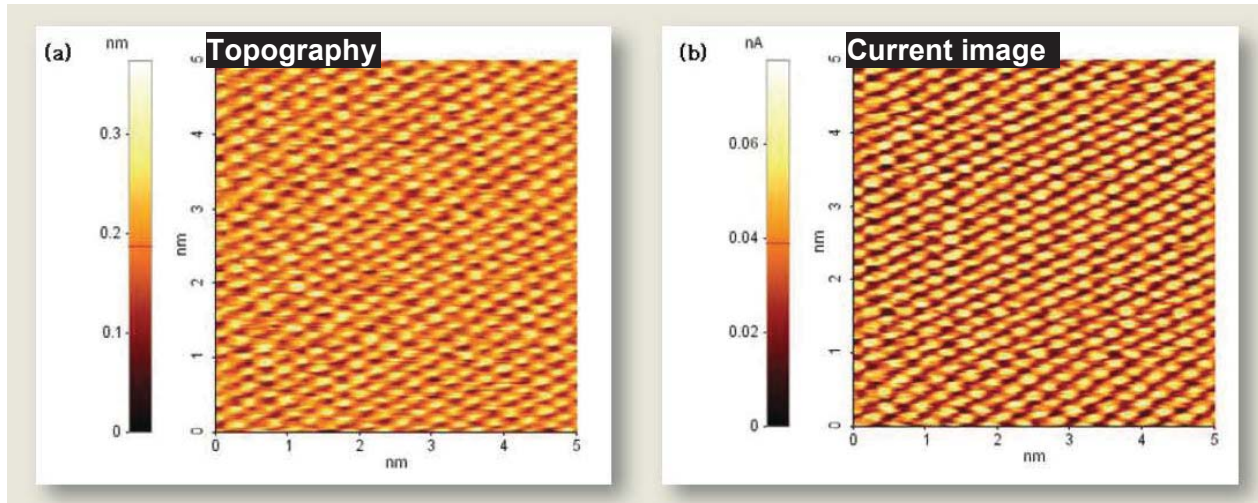
» In this way, the sample topography $z_{\text{sample}} = z_{\text{tip}}(x,y) + \text{const}$ can be directly measured **without** knowledge of the dependence of the tip-sample interaction $S(z)$ as a function tip-sample distance.



» **Limitation:** A **perfect topography reconstruction** requires that (i) the tip-sample interaction is homogeneous over the sample surface (i.e., does depend on the lateral position) and (ii) that the vertical repositioning of the tip is fast enough such that the tip can faithfully follow the surface morphology.

Example : STM imaging of highly ordered pyrolytic graphite

(a) Topography in constant current mode (b) Current image in constant height mode.

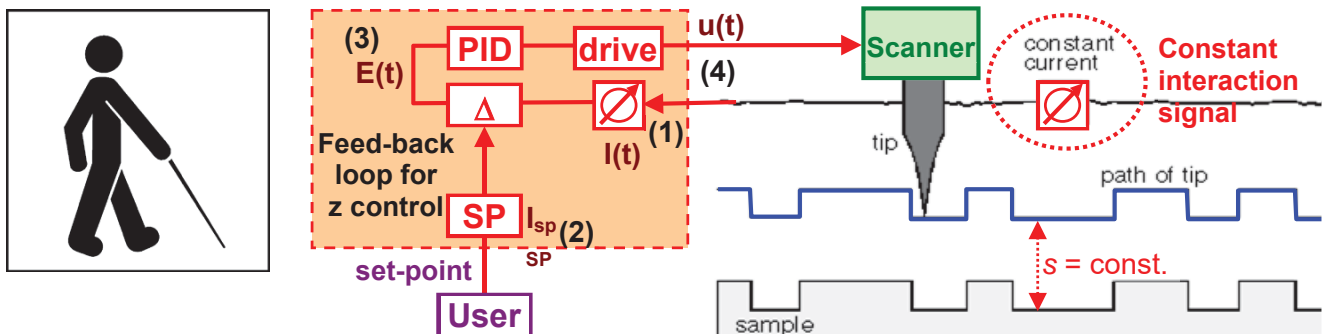


Generally: Samples are neither atomically flat nor physically homogenous:

Then, the SPM measurement corresponds to a superposition of topographic and interaction information. Separation possible only by application of spectroscopic techniques or multi-pass scan modes (see below).

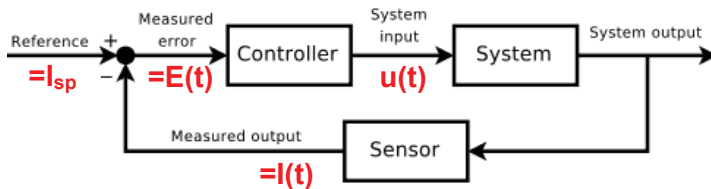
10.9 Feedback Loop and Scan Control

To perform a constant interaction scan, an **electronic feed-back control loop** is needed to keep the *tip-sample distance constant* during the scanning process and to reconstruct the surface topography.



Working principle of the feed-back Loop:

- **(1)+(2):** In the feed-back loop, the measured interaction signal $I(t)$ (1) is constantly compared to the user chosen set-point interaction I_{sp} value (2).
- **(3)** The difference between signal and set-point yields the so-called error signal $E(t) = I(t) - I_{sp}$ (3)
- **Case #1:** When the error signal is zero, the interaction strength is equal to the desired set point. Thus, the tip-sample distance has the correct value and the z- extension should be unchanged.
- **Case #2:** If the error signal is non zero, a drive voltage $u(t) = f(E(t))$ (4) must be generated and applied to the scanner to change the z-position of the tip until the measured interaction signal again reaches the desired set point value, i.e., until the error signal again goes to zero.
- If the error signal $E(t)$ is always \sim zero during the scanning process, then the tip follows exactly the surface topography $z_{st}(x,y)$. The topography is then simply given by: $z_{scanner}(x,y)$



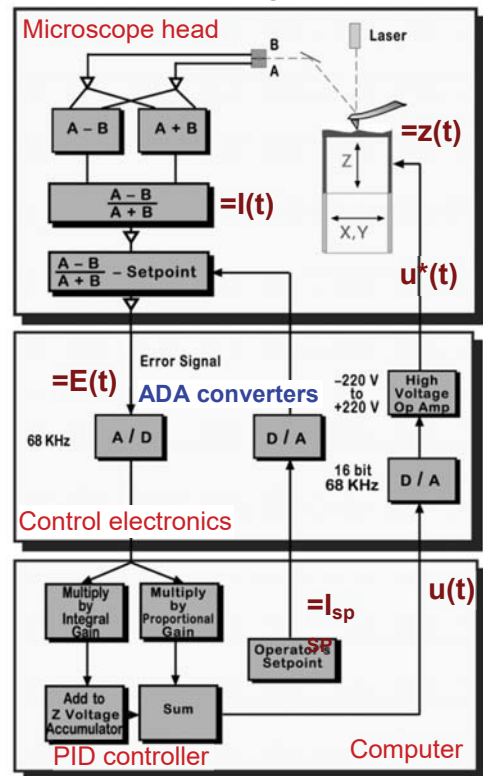
In general, a feed-back control loop consist of:

1. The **system** of which the state should be controlled. It is constantly driven by the drive signal but is also exposed to perturbations from the environment (e.g. vibrations) and by the sample topography (SPM).
2. a **sensor** that measures the status $I(t)$ of the system,
3. a reference channel that inputs the set-point value I_{sp} ,
4. a **comparator** that generates the **error signal** $E(t)$,
5. a feed-back **loop controller** that generates (or calculates) from the error signal a **drive signal** $u(t)$
6. an input of the drive signal to the **system** to change its state towards the desired set-point value I_{sp} .

Examples:

Temperature controller, pressure controller, velocity controller, position controller,

Example: Block diagram for AFM



10.9.1 Feedback Control Action

- ⇒ The **SPM feedback control loop** must continuously readjust the tip-sample separation in order to **keep the error signal as small as possible** during the scanning process.
- ⇒ The **controller** must therefore **generate** from the error signal **a scanner driving signal** $V_p(t) = f(E(t))$ that moves the SPM tip position up and down in such a way to minimize the error signal $E(t)$.

Limitation of the feedback action:

Practically, the **error signal** can never be kept **exactly** zero because the surface topography, i.e., the **surface height** $z_{sf}(x,y) = z_{sf}(t)$ **constantly changes** during the scanning process, and because the **reaction**, i.e., repositioning of the SPM tip can never be instantaneous and infinitely fast. This **delayed reaction** leads to an increase of the error signal whenever a change in surface height occurs.

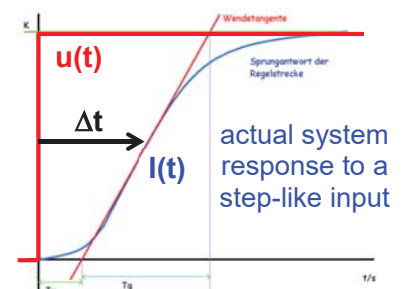
The **delayed reaction of the tip** is caused by several effects:

1. Mechanical **inertia** of the scanner, tip and sample,
2. Finite piezo response speed: Requires **charging of the electrodes**,
3. **RC delay times** of the electronic components, i.e., of the interaction signal detectors, pre- and high voltage amplifiers, etc. ...

Additional deviations from ideal scanning are caused by:

1. Unwanted mechanical excitations of scanner assembly, piezo elements and probe tip due to the rapid scanner motion in the vertical and lateral direction.
2. External electronic and mechanical noise coupled into the feedback loop and SPM gap.
3. Oscillations or instabilities caused by the feed-back loop itself !

This generally happens if the non-ideal feed-back parameters are applied.



10.9.2 PID Feed-Back Controller

The design and optimization of a feed-back loop and the control algorithms is the main issue of **control theory**, which is used in many different fields of engineering.

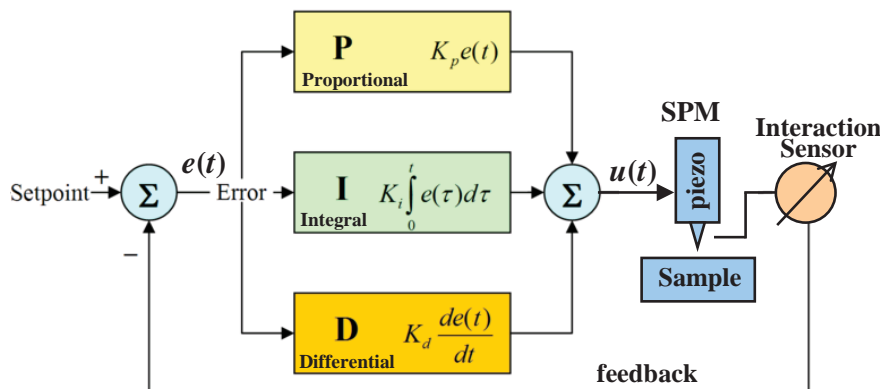
The **task** is to generate a drive signal $u(t)$ that adjusts the piezo extension based on the **known quantities** of the system, i.e., the momentary **error signal** $e(t)$ and the **output drive** $u(t-\Delta t)$ at time $t-\Delta t$.

PID controller

The most common feedback control design is the “Proportional-Integral-Derivative” (PID) controller. In this system, the control (drive) signal $u(t)$ is derived from the measured error signal $e(t)$ using the sum of three different components $u(t) = P(t) + I(t) + D(t)$ with the weighing factors K_P , K_I and K_D :

$$u(t) = K_P e(t) + K_I \int e(t) dt + K_D \frac{d}{dt} e(t)$$

Here: $u(t)$ is the z-voltage applied to the SPM scanner



(a) Proportional Control

The simplest solution is to set the drive signal $u(t)$ or $P_{out}(t)$ simply **directly proportional** to the

momentary **error signal**, i.e., $P_{out} = K_p e(t)$ which means that $z_{ip}(t) = K e(t)$

where K_p is the adjustable **proportional gain**, which is the tuning parameter of the P-control loop.

Basic properties:

A **high proportional gain** results in an **immediate reaction, i.e., large output change** for a given change in the error signal. A small gain results in a small output change and a less responsive (less fast) control action.

Problems:

- ❖ For pure proportional control, there **always remains a finite error signal** (= **steady state error**), i.e., the process value (interaction signal) never settles at its target set-point value !

This is because when the error signal is zero, the output P (piezo voltage) and thus the z-position of the SPM tip is set zero, which means the desired process value (= set-point of the tip-sample interaction) cannot be maintained.

As a result, a finite steady state error must remain to keep the drive signal non-zero.

- ❖ If the proportional gain **is too high**, the **system always becomes unstable** and starts to **oscillate**. If the proportional gain **is too low**, the control action becomes too slow when responding to system disturbances, i.e., to the sample topography.

Despite the steady-state offset, both tuning theory and industrial practice indicate that the **proportional term should contribute to the bulk of the output change** to achieve a good feedback system.

(b) Integral Control

The idea behind the integral control loop is to **change the output $\Delta I(t)$** , i.e., system reaction directly proportional to the momentary error signal $e(t)$, i.e.: $\Delta I_{out}(t) \sim e(t) \rightarrow dI_{out}(t)/dt = K_i \cdot e(t)$

In simple terms, this means that if the error signal is zero, the system keeps in its current state, and if not, its speed of reaction is directly proportional to the magnitude of the error signal, i.e., large error means fast reaction, small error means slow reaction.

By integration over time, the actual output value I_{out} is derived as:

$$I_{out}(t) = K_i \cdot \int_0^t dI_{out}/d\tau \cdot d\tau = K_i \cdot \int_0^t e(\tau) \cdot d\tau$$

Thus, according to this algorithm the actual drive signal $I_{out}(t)$ is proportional to the **time integrated error signal**. K_i is the adjustable **integral gain** and also the integration time can be varied.

Basic properties:

1. The integral term adds to the momentary output a value proportional to the momentary error:

Thus: $I_{out}(t) = K_i \cdot \int_0^{t-dt} e(\tau) \cdot d\tau + K_i \cdot e(\tau)$ i.e., $I_{out}(t) = I_{out}(t-dt) + K_i \cdot e(\tau)$

The new output at time t is obtained by adding the just measured $K_i e(t)$ to the previous output at $(t-dt)$.

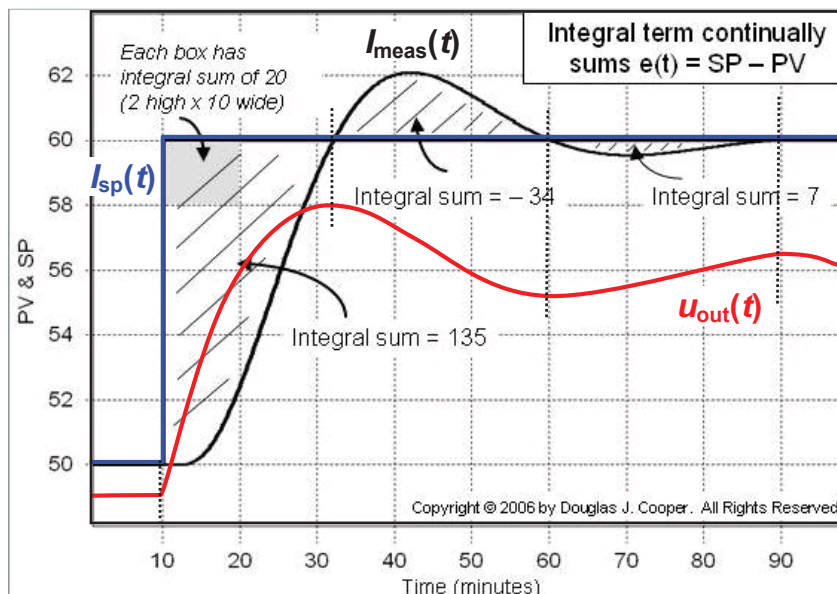
2. The integral control term completely **eliminates the residual steady state error**!

Reason: The output I_{out} is **changed only** if the error signal is non-zero. When the target value is reached the drive signal I_{out} is kept constant. Thus, the integral term always drives the process towards the correct set point.

3. **Drawback:** Because the integral term is proportional to the **accumulated errors** from the past, a quite **large delay** and **overshoot** over the set point value usually occurs and response is slow.

Example for the action of a P+I controller:

$$u(t) = MV(t) = K_p e(t) + K_i \int_0^t e(\tau) d\tau$$



(c) Derivative Control

Idea: To reduce the overshoot, an additional term is added to the output $u(t) = D_{out}(t)$ that is set proportional to the time derivative (slope) of the error signal de/dt :

$$D_{out} = K_d \frac{de}{dt}$$

Thus, when the system approaches the set-point very fast, the drive signal is reduced already before the set-point is actually reached. The strength of this contribution is given by the derivative gain K_d .

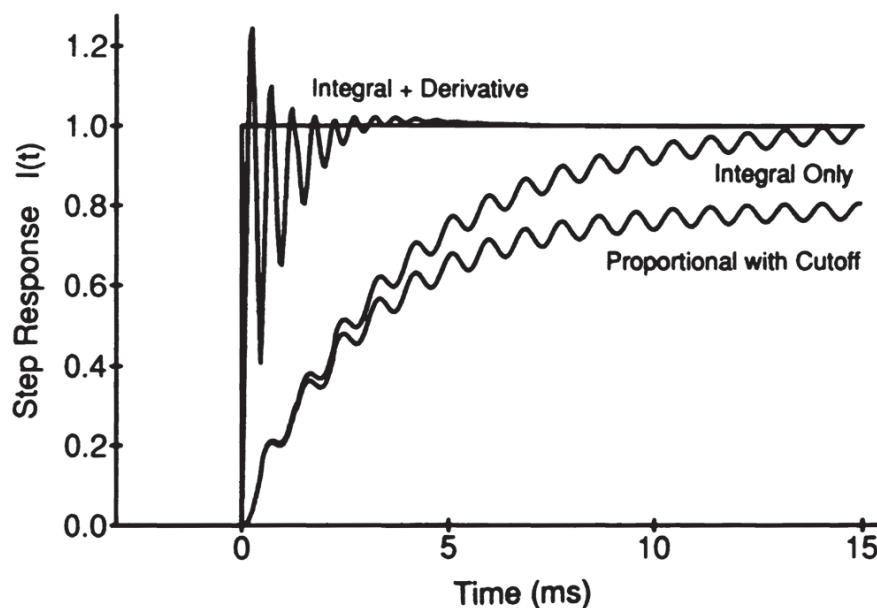
Basic properties:

1. The derivative control term can **improve the dynamical behavior** of the system, because the time derivative takes into account the speed at which the set point of the system is approached. If the speed is very fast, then the derivative term can reduce the control output already **before** the actual set-point value is reached.

Thus, the derivative term anticipates the response of the control system (= "**look-ahead**" gain) and **reduces the overshoot** of the system.

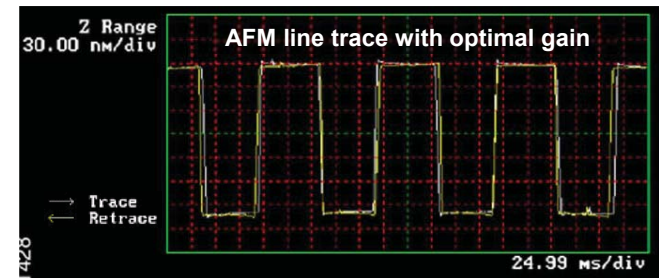
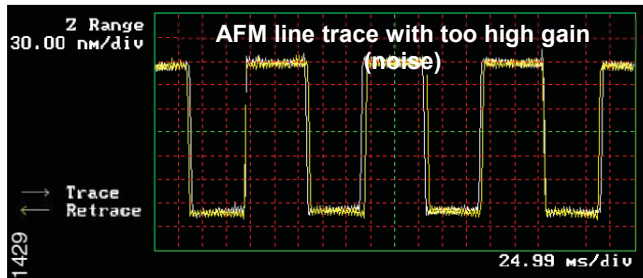
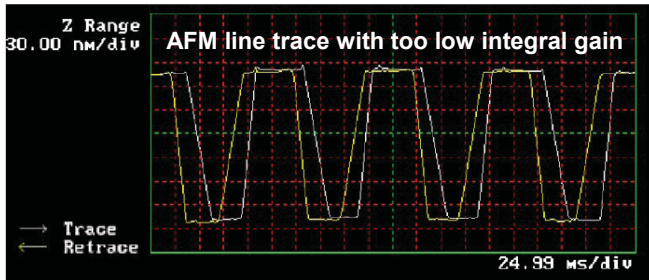
2. A derivative control term **alone never leads to a stable control system**. It can be used only in *conjunction* with a proportional or integral control term.
3. Although derivative control improves the response time of the system, it also makes it more **unstable** because even small perturbations and noise are strongly amplified in the feed back loop. As a result, in most cases the derivative gain is set to zero in most SPM applications.

Comparison of the response for different PID controllers



Practical Example: AFM line scans of a calibration grating with different scan parameters

White lines: Forward scan direction ("trace"). Yellow lines: Backward scan direction ("retrace")



- **General conclusion:** Optimum feedback parameters depend on
 - (a) SPM scan head construction (resonance frequency)
 - (b) Scanning speed,
 - (c) the sample topography (lateral size and height of surface features)
 - (d) AFM: Force constant of cantilever force sensor
- Must be optimized for a given sample and scan conditions.

10.10 Non-Contact / Tapping Mode AFM

In this operation modes the cantilever is used as a driven oscillator (**tuning fork**) that is excited into high frequency vibration by an piezo actuator mounted underneath the cantilever chip.

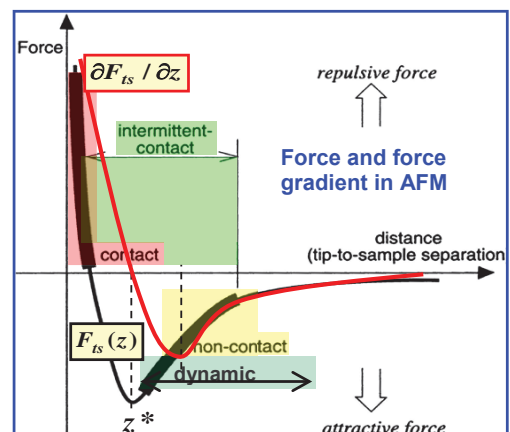
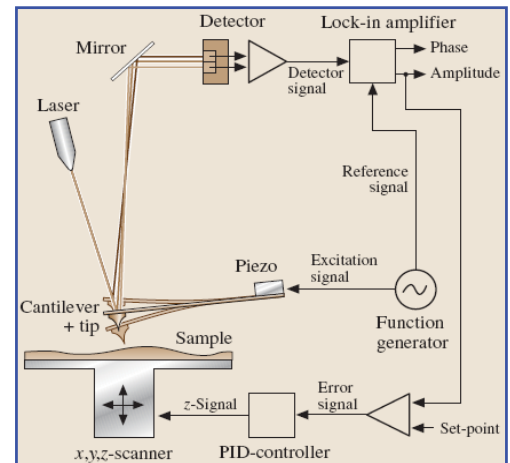
Interaction sensing: When the tip interacts with the sample the oscillating properties (**resonance frequency, amplitude and phase**) slightly change and these changes can be detected with high sensitivity using lock-in techniques. This provides an alternative measure of the-sample interaction compared to measuring only the force interaction.

Main operation modes:

- **Tapping/intermittent contact mode** (large amplitude, intermittent contact between tip and sample)
- **Non-contact mode AFM** (@large tip-sample distance)
- **Derivative force imaging** (small oscillation amplitudes)

Detection schemes:

- **Amplitude detection:** Excitation with fixed excitation frequency + measurement of change of amplitude.
- **Phase detection** (fixed frequency excitation): Measurement of the phase difference between the excitation and the detector signal.
- **Frequency detection:** Measurement of frequency shift due to the interaction (variable frequency excitation).



10.10.1 Cantilever as Driven Damped Harmonic Oscillator

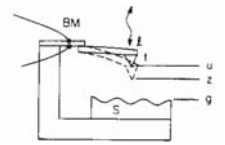
Here, we consider the cantilever as **damped harmonic oscillator** driven by a **periodic driving force** with an amplitude $F_{d,0}$ and a drive frequency ω .

Equation of motion:

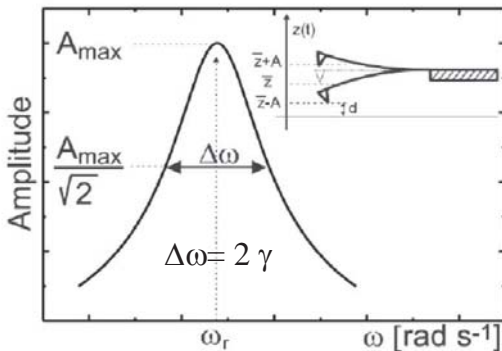
$$F_{tot} = F_{elastic} + F_{friction} + F_{drive} = m \cdot a$$

k = force constant, b = damping constant

$$m \cdot \ddot{x} + b \cdot \dot{x} + k \cdot x = F_{d,0} \cos(\omega t + \theta_0)$$



Steady state solution (resonance curve $A(\omega)$ of free-air eamped oscillator)



$$k A_{exc} \cos(\omega t) = \frac{k}{\omega_0^2} \ddot{z}(t) + \frac{k}{\omega_0 Q} \dot{z}(t) + k z(t) \quad \omega_0 = \sqrt{\frac{k}{m}}$$

$$z(t) = \bar{z} + A \sin(\omega t)$$

$$Q = A_{max}/A_{exc} = \omega_r / 2\Delta\omega = \omega_r / 4\gamma \quad Q = \text{quality factor}$$

$$A_0 = \frac{A_d Q \omega_0^2}{\sqrt{\omega^2 \omega_0^2 + Q^2 (\omega_0^2 - \omega^2)^2}}$$

$$\phi = \arctan \left(\frac{\omega \omega_0}{Q (\omega_0^2 - \omega^2)} \right)$$

A_0 = cantilever amplitude

ϕ = phase with respect to drive signal

$$\omega = \omega_r = \sqrt{\omega_0^2 - 2\gamma^2}$$

Resonance frequency

On resonance, the phase shift

$$\phi = \frac{\pi}{2}$$

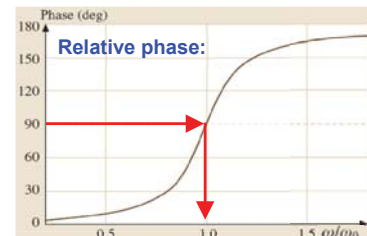
$$\omega_0^* = \omega_0 \sqrt{1 - \frac{1}{2Q^2}}$$

Far below resonance

$$\omega \ll \omega_r, \quad \phi \rightarrow 0$$

Far above resonance

$$\omega \gg \omega_r, \quad \phi \rightarrow \pi$$



10.10.2 Oscillating Cantilever Interacting with a Sample Surface

When the **tip interacts with the sample**, an additional force F_{ts} acts on the tip when it is in close vicinity of the sample surface. As a result, the **oscillation properties slightly change**.

⇒ The interaction strength is thus sensed by measuring the **changes** in the **resonance frequency** $\Delta\omega$ and/or **changes in the oscillation amplitude** ΔA and **phase** $\Delta\phi$ as shown below. These changes can be used alternatively for the measurement of the cantilever deflection.

These resulting scan modes are called tapping or intermittent contact or noncontact scan modes

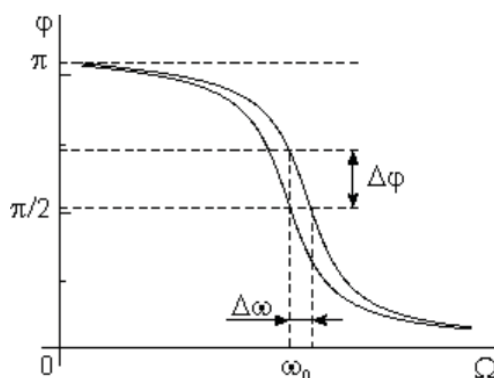


Fig. 4.2. Variation of the oscillations phase with resonant frequency.

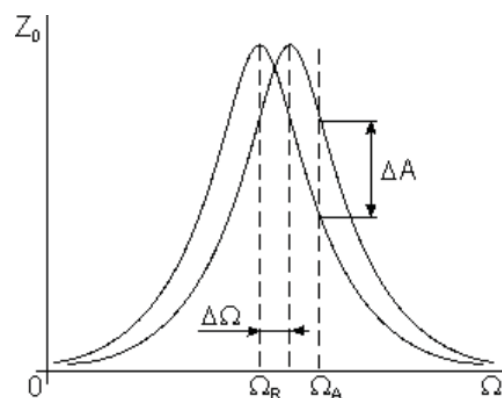
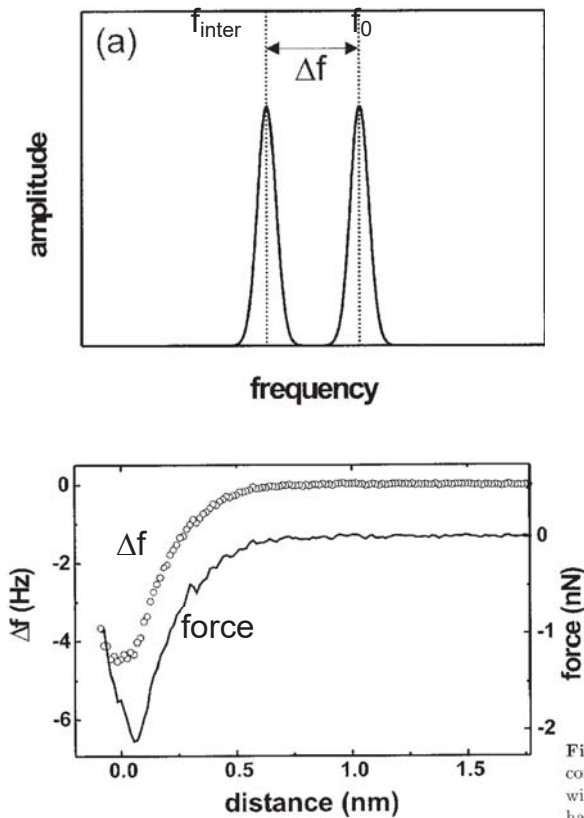


Fig. 4.3. Variation of the oscillations amplitude with resonant frequency.

- ⇒ In general, if the interaction is dominated by repulsive forces, the resonance frequency **increases** as the tip approaches the sample because the cantilever is pushed back more strongly.
- ⇒ On the contrary, when attractive forces dominate the resonance frequency is **lowered**.

(a) Small amplitude oscillation approximation = Force Gradient Detection



Change of resonance frequency due to a **tip-sample force gradient**:

$$k_{\text{total}} = k + k_{\text{ts}} = k - \frac{\partial F_{\text{ts}}}{\partial z}$$

$$\omega^2 = (\omega_0 + \Delta\omega)^2 = k_{\text{total}}/m^* = \left(k + \frac{\partial F_{\text{ts}}}{\partial z}\right)/m^*$$

$$\frac{\Delta\omega}{\omega_0} \approx -\frac{1}{2k} \frac{\partial F_{\text{ts}}}{\partial z}$$

Δf is proportional to the force gradient !

For **small excitation amplitudes**, the **frequency shift Δf** is directly **proportional** to the **tip-sample force gradient** !

Fig. 3.21. Conversion of a Δf vs. distance curve into a force vs. distance curve according to the iterative procedure introduced by Dürig [212]. The data are recorded with a silicon tip approaching a Si(111)7×7 surface. The long-range contribution has been subtracted

(b) Large amplitude excitation

For large oscillation amplitudes, calculation of the **frequency shift** due to the tip-sample force gradient has to be replaced by an **effective force gradient** that is averaged over the whole oscillation period with a certain weighing factor:

$$k_{\text{eff}}(z) = \frac{\sqrt{2}}{\pi} A^{3/2} \int_z^\infty \frac{F(x)}{\sqrt{x-z}} dx$$

This yield the **frequency shift**:

$$\Delta f = \frac{f_0}{\sqrt{2\pi k A^{3/2}}} \int_z^\infty \frac{F(x)}{\sqrt{x-z}} dx$$

The frequency shift thus **depends on the amplitude A of the oscillation** in this case.

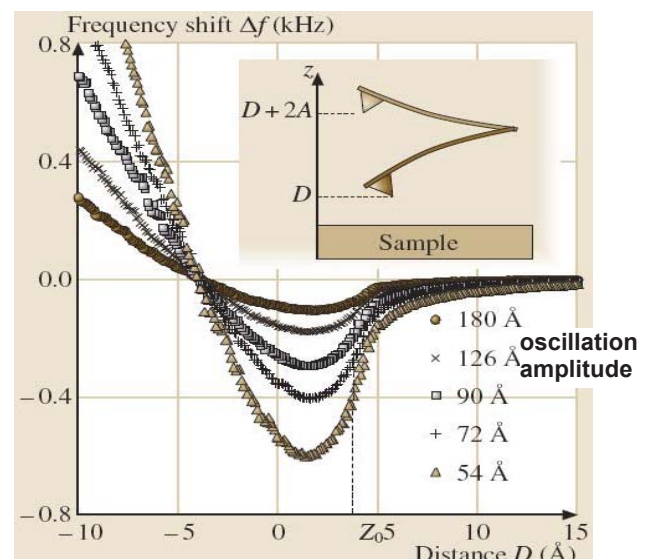
The frequency shift is generally larger for small amplitudes.

Reason: For large amplitudes most of the time only small force gradients act on the tip

$$k_{\text{ts}}(z) = \partial F / \partial z|_{z_0}$$

$$k_{\text{eff}}(z) = \frac{2}{\pi A^2} \int_z^{z+2A} F(x) g\left(\frac{x-z}{A} - 1\right) dx$$

with $g(u) = -\frac{u}{\sqrt{1-u^2}}$.



10.10.3 Oscillation Detection Modes: Amplitude vs Frequency Detection

(a) **Amplitude Detection**: = Excitation at **constant excitation frequency** f_{exc} close to f_{res}
Measurement of **amplitude change** ΔA using lock-in technique.

(b) **Frequency modulation mode**: = Excitation frequency is kept **tuned to resonance** and amplitude kept constant. Measurement of **frequency change** Δf relative to free-air resonance frequency

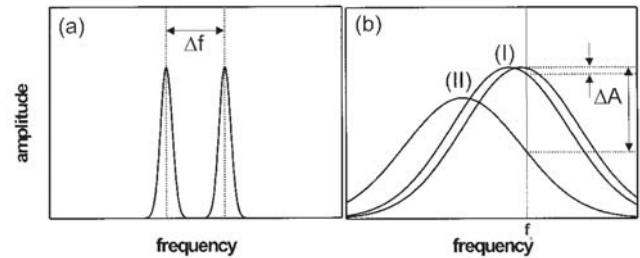
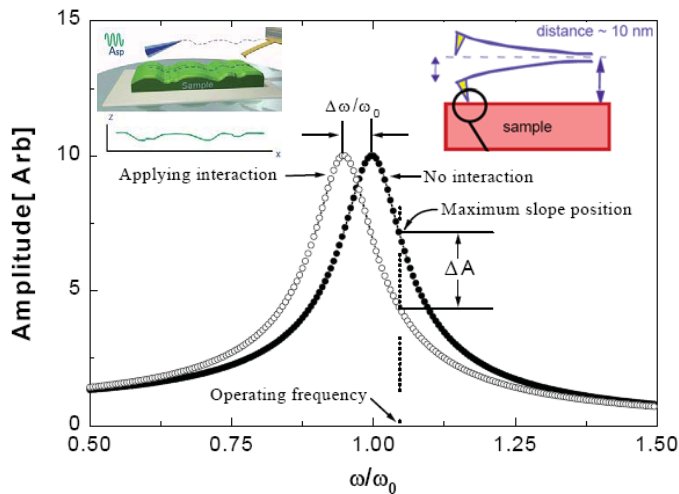


Fig. 3.7. Two dynamic modes for the detection of tip-sample interactions. In dynamic force microscopy (a), the shift in frequency caused by the tip-sample interaction is detected. The oscillation is driven at the actual eigenfrequency of the cantilever. This mode is mainly applied in vacuum, where high Q -factors allow a precise determination of the resonance frequency. In the intermittent contact mode (b), the change in amplitude is detected at a fixed frequency f_0 . This mode is suitable for systems with low Q -factors, where the amplitude changes fast enough upon tip-sample interactions. The decrease in amplitude at f_0 may be due either to a frequency shift (I) or to an additional decrease in the total amplitude due to damping (II)

10.10.4 Intermittent Contact (Tapping) versus Non-Contact Mode

Tapping mode (= intermittent contact) AFM

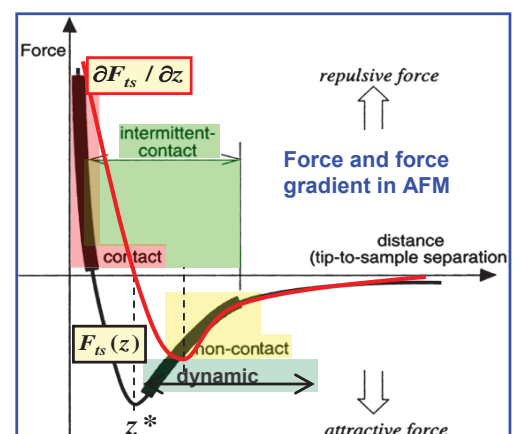
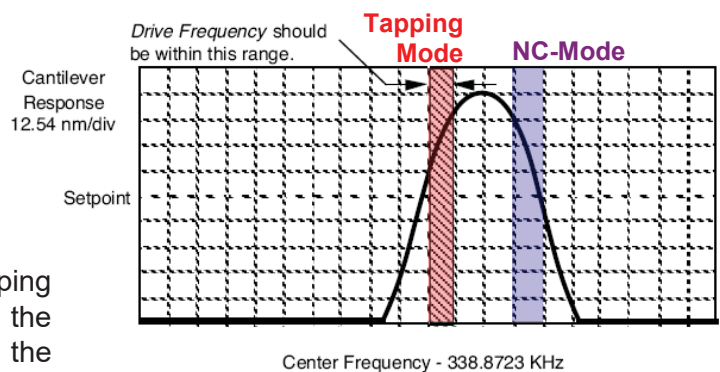
In this operation mode, the **excitation frequency** is **set slightly below the resonance frequency** of the free cantilever and the amplitude set-point for scanning at a value lower than the amplitude of the free cantilever at the excitation frequency.

As the tip comes into the **contact regime** (tapping on the sample), the resonance curve shifts to the right hand side to higher frequencies and thus, the cantilever amplitude at the drive frequency is reduced until the set-point value is reached.

Non-contact mode (far distance attractive force regime)

In NC-mode AFM, the **excitation frequency** is **set slightly above the resonance frequency** of the free cantilever and the amplitude set-point for scanning at a value lower than the amplitude of the free cantilever at this excitation frequency.

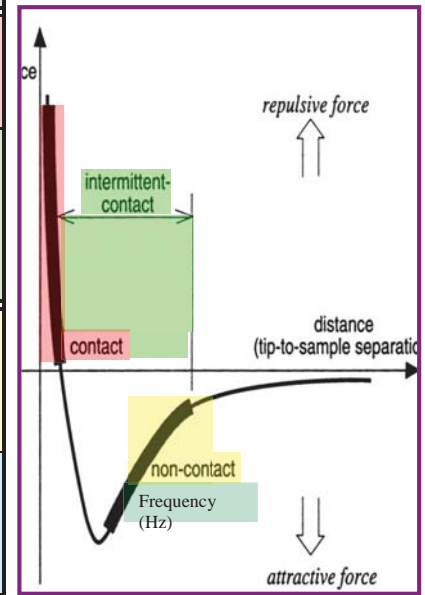
As the tip comes in the non-contact regime, the resonance curve shifts to the left hand side to lower frequencies because the attractive force retards the cantilever oscillation. Thus, at the fixed excitation frequency, the cantilever amplitude is reduced until the set-point value is reached.



10.10.5 Comparison of the different AFM Imaging Modes

Table: Operation modes in atomic force microscopy

Mode	Advantages	Disadvantages
Contact Mode <i>Static (DC)</i>	High lateral resolution (Å) simple operation simple interpretation	Large tip wear due to strong tip-sample interaction, limited force resolution
Contact Mode <i>Dynamic (AC)</i> intermittent or tapping mode	Highest spatial resolution (atomic) and sensitivity, high force resolution (pN) low noise, high stability reduced sample damage	More advanced instrumentation
Noncontact Mode-Static (DC)	Nondestructive: No tip wear, and no sample damaging, sensitivity to long range forces (MFM)	Poor spatial and force resolution (~10nm) unstable operation very sensitive to drifts
Noncontact Dynamic (AC)	Nondestructive higher sensitivity as DC, sensitivity to long range forces (MFM)	Poor spatial resolution (~10nm)

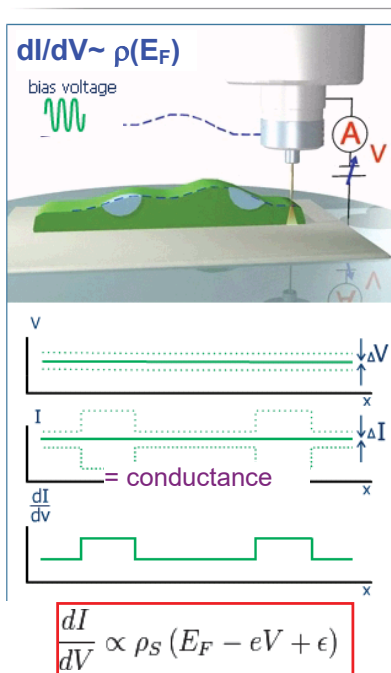


10.11 AC-Modulation or Dynamic Scan Modes

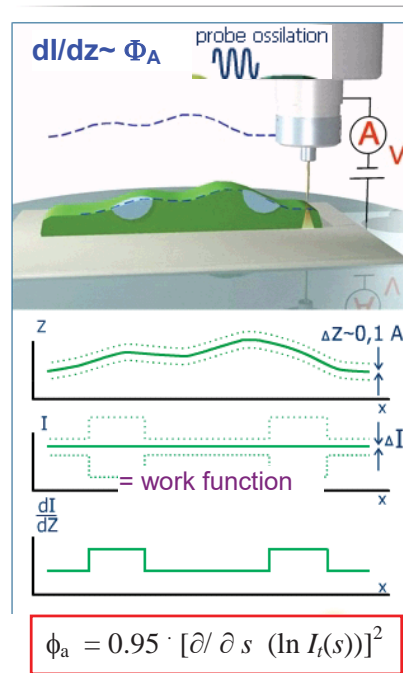
In these scan modes, the **control parameters** such as U_t or z are **modulated by a high frequency excitation** and the resulting modulation of the interaction signal is detected using a highly sensitive lock-in technique. This gives access to additional properties of the tip-sample interactions. Examples:

STM: Conductance and Barrier Height Imaging

Density of States imaging

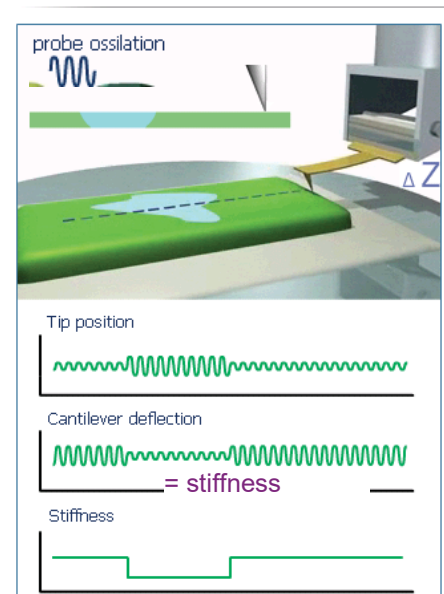


Barrier Height imaging



AFM: Force Modulation Imaging

Force Modulation mode



Example: Tunneling Conductance: dI/dV Maps

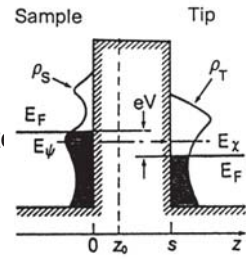
Under the assumption of $M_{\mu\nu}$, and $\rho_T = \text{const.}$ the tunnelling current is given by:

The **derivative of the tunnelling current** with respect to the tunnelling voltage dI/dV , i.e., the **tunnelling conductance** is then given by:

$$\frac{dI}{dV} \propto \rho_S(E_F - eV)$$

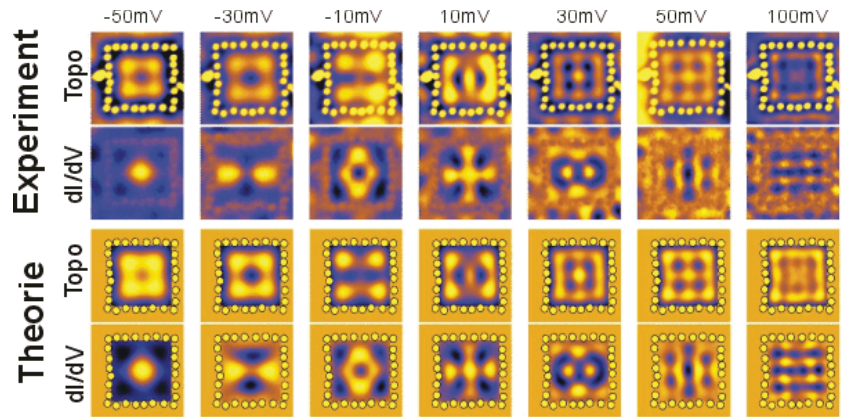
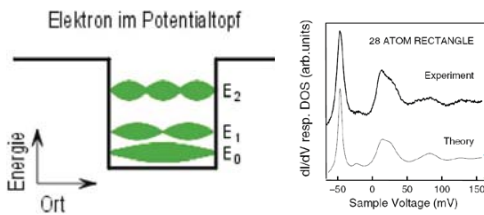
Thus, the tunnelling conductance is directly proportional to the local density of states (LDOS) of the sample at a given energy $E = eV$ with respect to the Fermi Level E_F !

Therefore, tunnelling conductance images recorded at different bias voltages correspond to the LDOS distribution of the sample at different electron energies.



Example:

Array of 28 Mn atoms on Ag (111) forming a quantum coral of $\approx 90 \times 100 \text{ \AA}^2$, in which the 2D surface state of Ag(111) is quantum confined.



Imaging of conductance over the surface, shows different patterns of the confined electron wave function within the quantum coral: At higher energy (higher voltage), the number of nodes (minima/maxima in dI/dV) within the coral increases.

(Kliewer et al., 2001 New J. Phys. 3, 22)

Example for Force Modulation AFM imaging

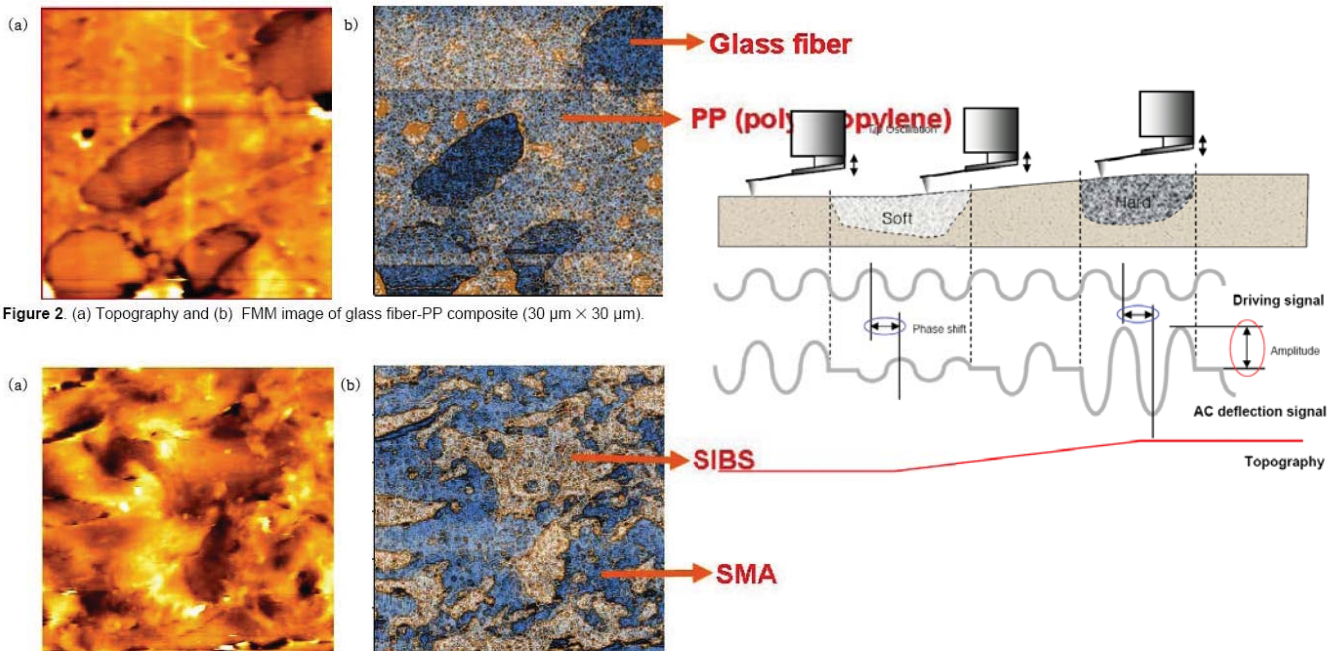


Figure 2 (a) Topography and (b) FMM image of glass fiber-PP composite (30 $\mu\text{m} \times 30 \mu\text{m}$).

Figure 3 (a) Topography and (b) FMM image of bland polymer : SIBS 1027 60% +SMA 14 40% (30 $\mu\text{m} \times 30 \mu\text{m}$).

10.12 Hybrid Scan Modes

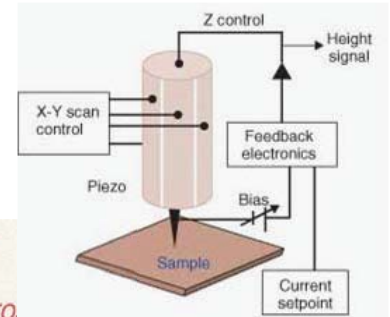
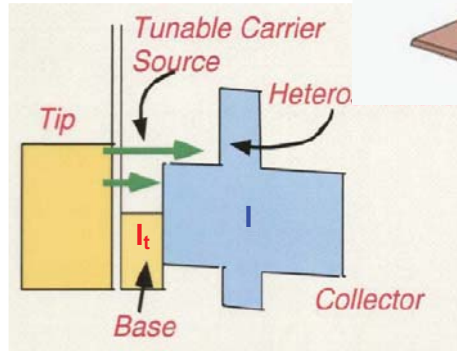
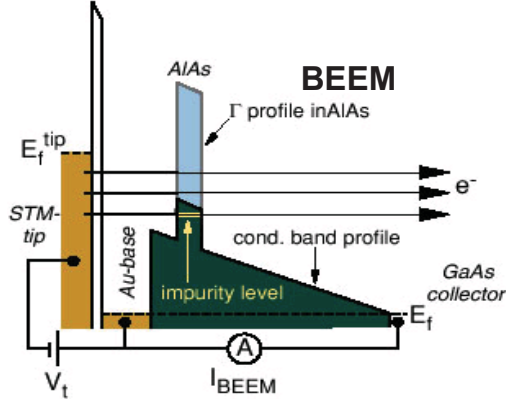
In hybrid scan modes, **several interactions** are measured simultaneously during imaging process. One interaction signal (typically the force or tunneling current) is used to keep the tip at a constant height / separation. The other interaction signals at this constant separation are used to measure local physical properties of the sample such as frictional force, capacitance, conductance, etc. :

Examples for STM

- ❖ **BEEM-STM**: Ballistic electron emission microscopy:

Feedback signal = tunneling current,

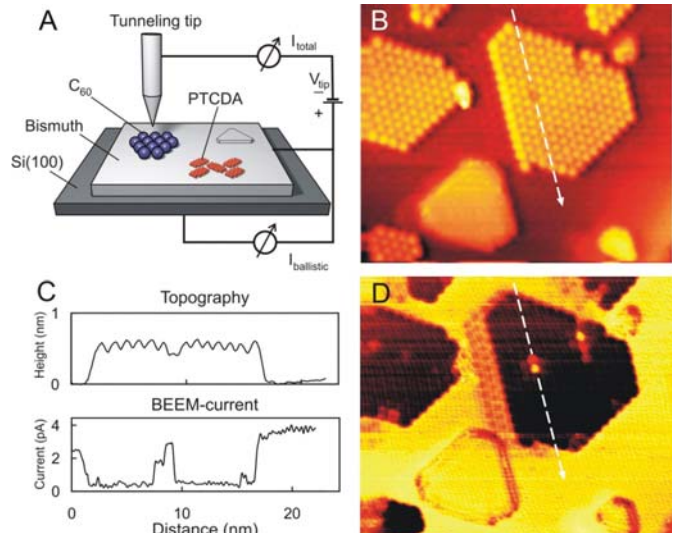
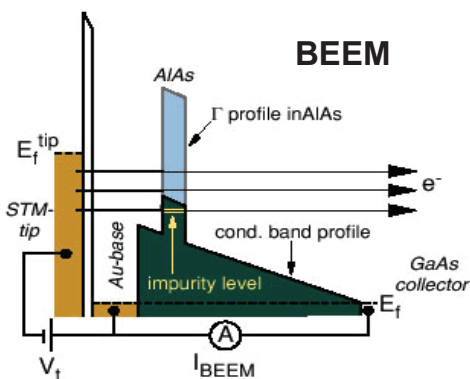
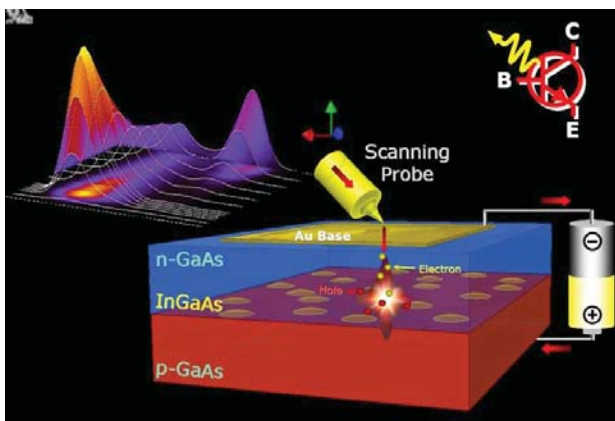
BEEM Signal: Ballistic electron current to a **subsurface collector**.



- ❖ **Conductance / Work function imaging STM**:

Feedback signal = tunneling current, **Measured signal**: dI/dV , dI/dz (...see previous section)

Ballistic Emission Electron Microscopy (BEEM) – Example for Double Detection Method



A. Bannani et al. Science 315, 2007:1824

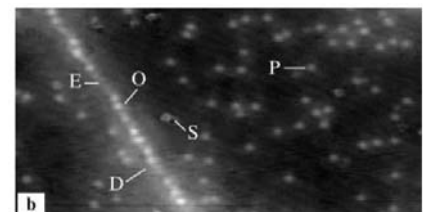
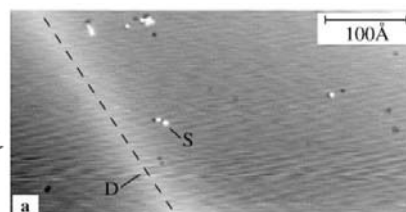


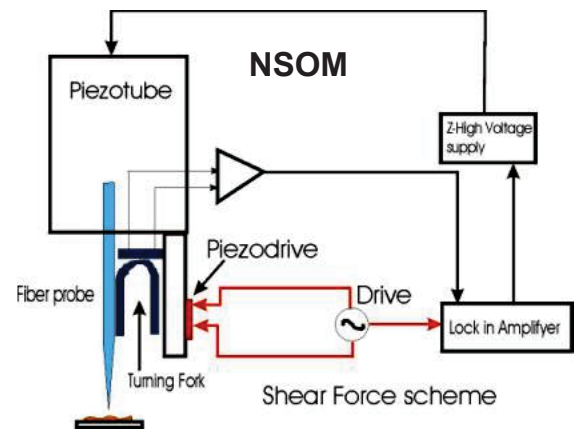
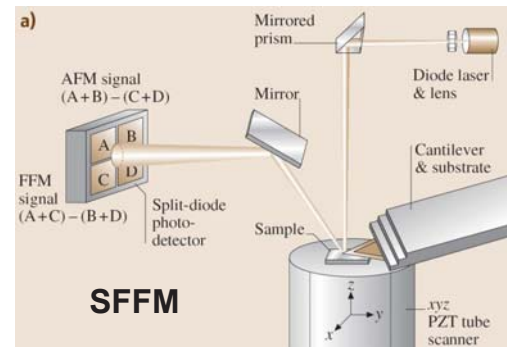
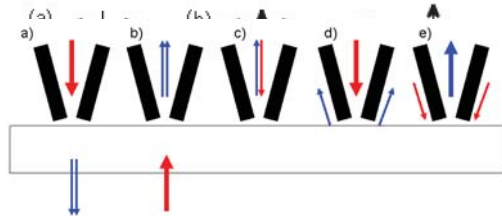
Fig.1. a STM topography image and b corresponding BEEM image of a 28 Å-thick $\text{CoSi}_2/\text{n-Si}(111)$ film, recorded with $V_t = -1.2$ V and $I_t = 20$ nA. Interfacial point defects have been trapped within the dislocation D. Empty and occupied sites in the dislocation are designated by E and O.

Further Examples of Hybrid Scan Modes

Measurement of **several interactions** simultaneously during imaging process.

Examples for AFM and NSOM

- ❖ **SFFM**: Scanning frictional force microscopy
Feed-back signal = repulsive AFM force,
Measured signal = lateral frictional force on AFM tip.
- ❖ **SCM**: Scanning conductance or scanning capacitance microscopy
Feed back signal = AFM force,
Measured signal = electrical conduction or capacity of tip with respect to sample.
- ❖ **NSOM**: Near field scanning optical microscopy
Feedback signal = non-contact AFM, i.e., the optical fiber vibration resonance frequency,
Measurement signal = local photoluminescence, local optical transmission from or to the optical fiber.



Lateral (Frictional) Force Microscopy – Double Detection Method

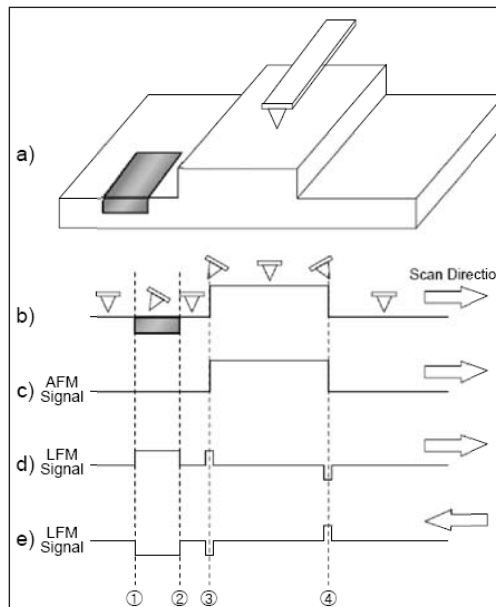
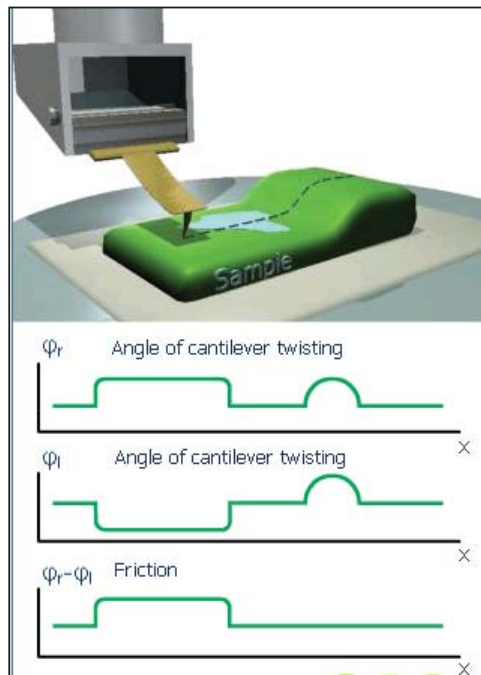


Figure 2. AFM and Lateral deflection signals of the cantilever from changes in surface friction and profile slope

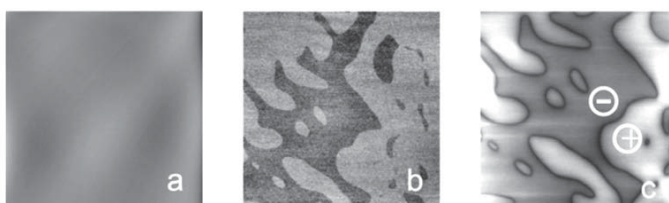
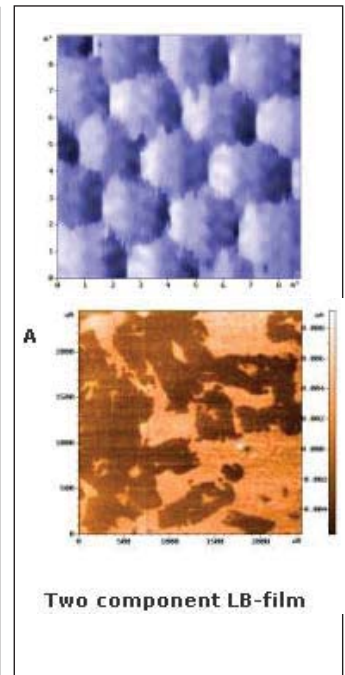
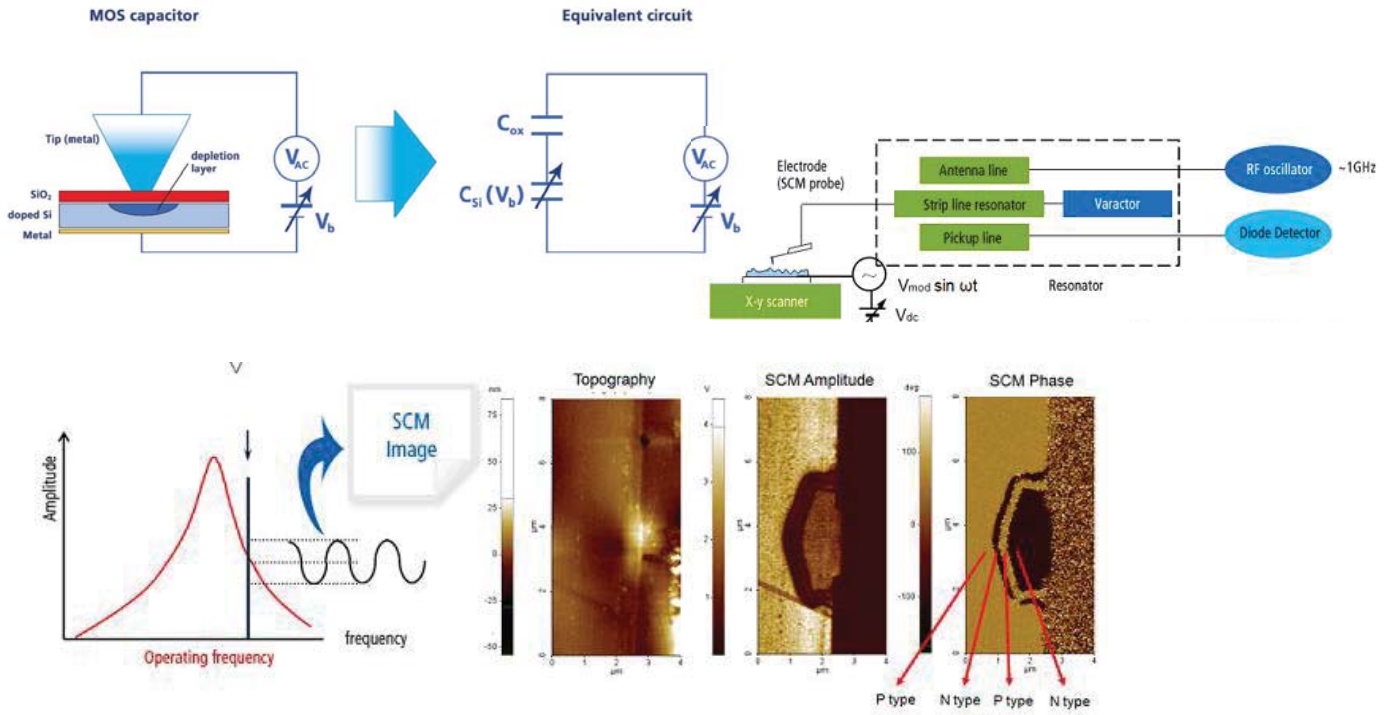


FIGURE 18.7 (a) Topographical image of GASH(0001) (image size: 30 μm × 30 μm). The surface is featureless and without any steps. (b) Friction force map of the same surface spot as in (a) (slight zoom-out; image size: 40 μm × 40 μm). A well-expressed contrast is visible. (c) Image acquired with electrostatic force microscopy at the same surface area as in (a), showing the structure and absolute sign of the ferroelectric domains. By comparison of (b)

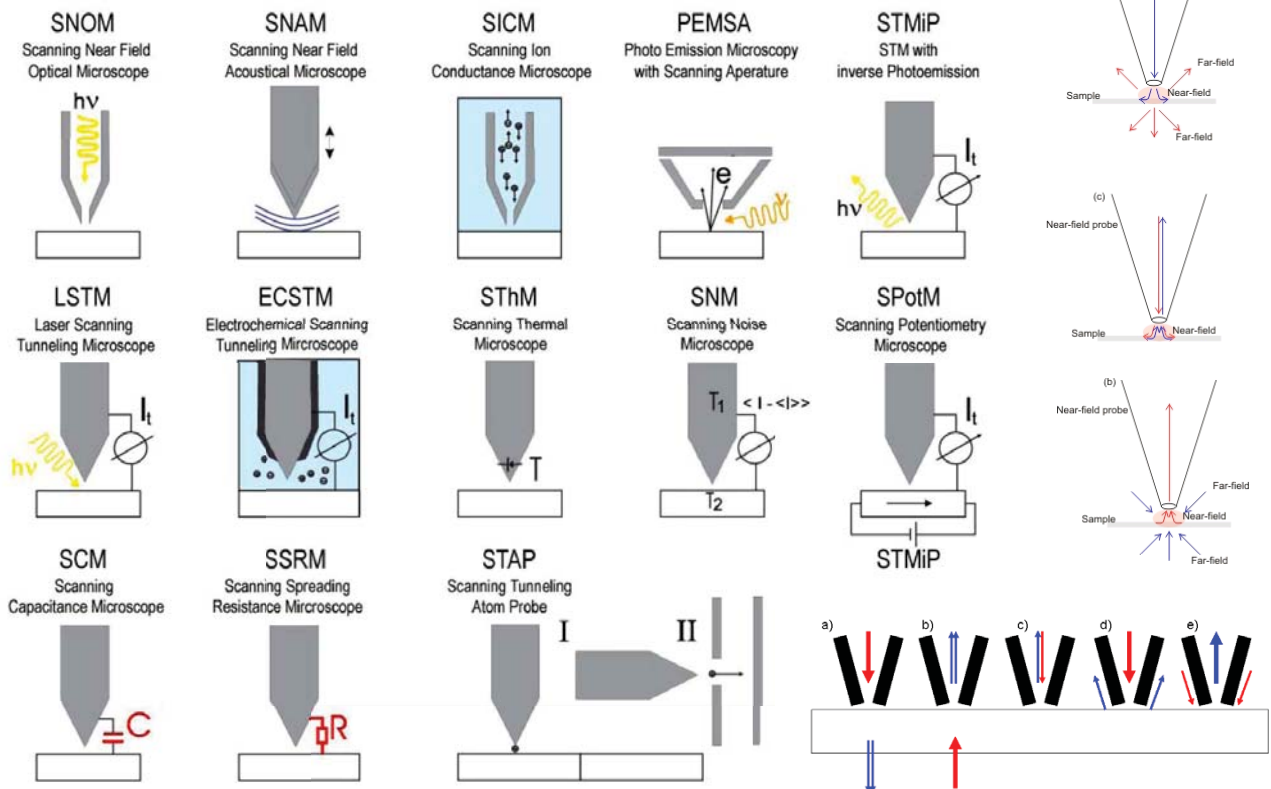
Scanning Capacitance Microscopy (SCM)



By detecting the capacitance change between a cantilever and a sample, SCM can image carrier density or dopant concentration.

Additional Examples for Hybrid SPM Scan Modes

Measurement of additional interactions signals during the scanning process



10.13 Multi-Pass Methods

Aim: *Separation between different interaction signals* (different *contributions* to the interaction signal).

This is achieved by scanning each line of sample twice:

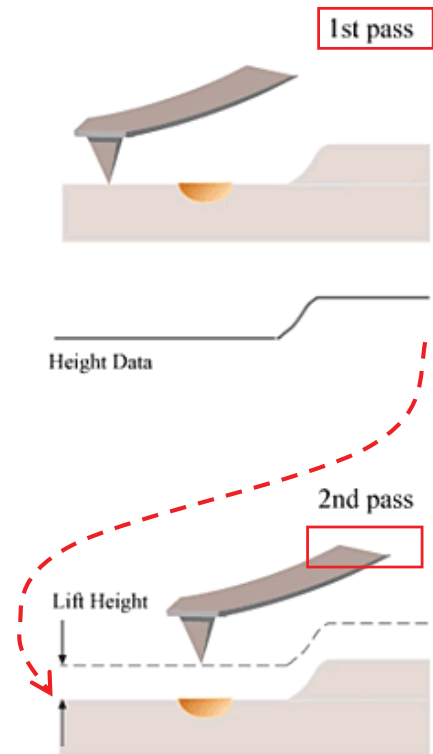
- ❖ **First scan** = Yields topography profile,
- ❖ **Second scan** = Tip is moved over the surface at a selected *constant distance* along the profile recorded in the first scan.

⇒ Since the signals during the second scan are recorded at constant sample distance, the signal recorded during the second scan contains exclusively *contributions from non-topography related interactions*. Thus, *pure material contrast* can be obtained.

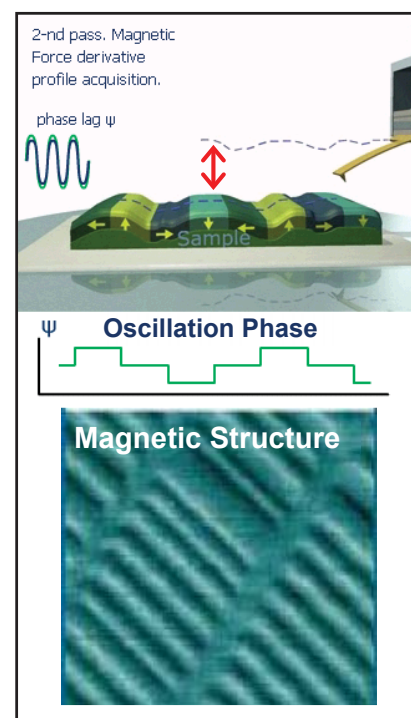
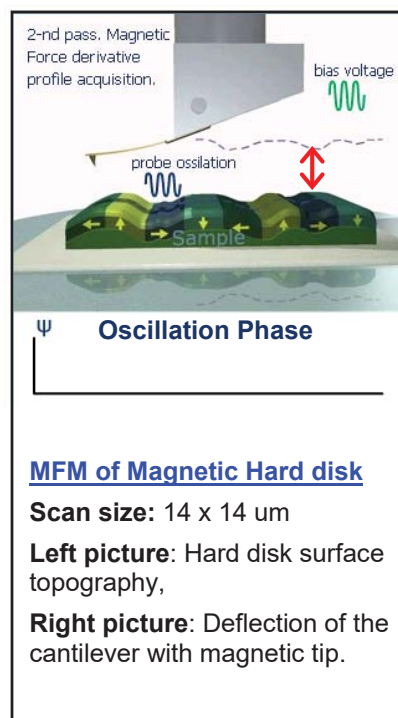
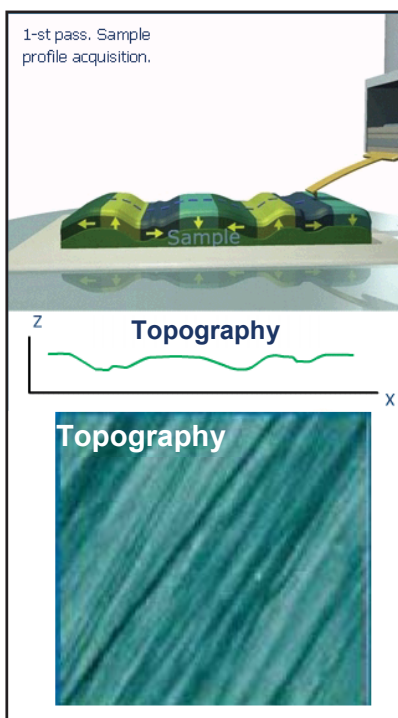
⇒ The selectivity of the signal can be enhanced by using an optimized *lift height* used during the second scan

Multi-pass scan methods are predominantly used for discrimination between different force interactions with different distance **dependences**.

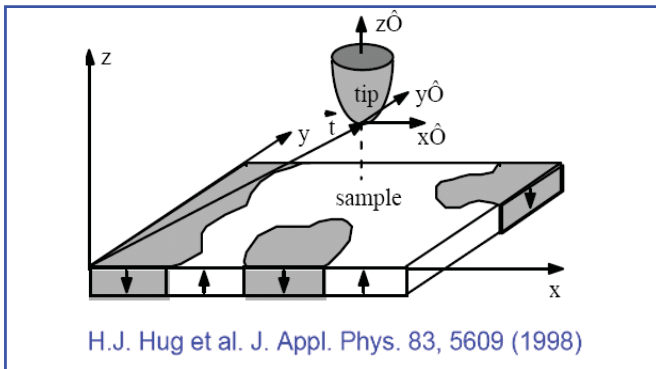
Example: Magnetic force microscopy.



Example: Magnetic Force Microscopy using Double Pass Lift Height Method



Magnetic Force Microscopy (MFM)



$$F_z(\vec{t}) = -\mu_0 \int \vec{M}_{tip}(\vec{r}) \cdot \frac{\partial}{\partial t_z} \vec{H}_{sample}(\vec{r} + \vec{t}) d^3r$$

Contrast formation in direct space

$$F_z(\vec{r}) = \int_{V_{tip}} \frac{\partial H_z(\vec{r} + \vec{r}')}{\partial z} \cdot M_{tip}(\vec{r}') d^3r'$$

Point-pole tip models

$$F_z(\vec{r}) = q_{tip} \cdot H_z(\vec{r}) + p_{tip,z} \cdot \frac{\partial}{\partial z} H_z(\vec{r})$$

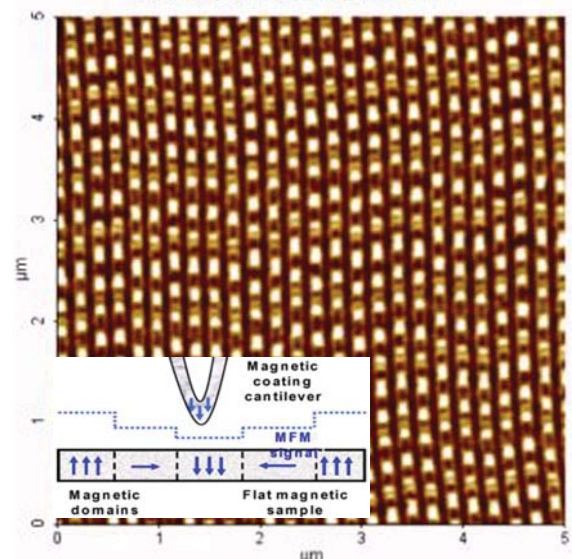
Image simulation requires a 3d-integration at each position of the tip & knowledge of M_{tip} .
Quantitative image interpretation not possible!

Quality of point-pole tip models not sufficient, because q_{tip} and p_{tip} depend strongly on spatial wave-length of H-field!
Quantitative image interpretation not possible!

MFM simultaneously measures both topography and magnetic properties of sample. Using a cantilever coated with magnetized metal layer, spatial variation of magnetic domains can be observed, which gives more information than optical measurement such as magneto-optical Kerr effect.

MFM Image of Hard Disk Drive

Bit size: 200 x 200 nm



12GB Small Form Factor HD - 25bit/μm²
(scan size : 5 x 5 μm)

10.14 Summary

1. **In scanning probe microscopy**, the surface of a sample is scanned with a microscopically sharp **probe tip** at a distance of 1... 50 Å away from the surface. The **tip-sample distance** is controlled by measuring the strength of the tip-sample interaction.
2. **Several different types of interactions** occur between the tip and sample surface: Quantum mechanical, repulsive / attractive forces, dipolar & van der Waals forces, tunneling, etc. . The type of utilized interaction determines the SPM technique.
Main techniques: Scanning Tunneling Microscopy (STM), Scanning (Atomic) Force Microscopy (SFM/AFM), Scanning Near Field Optical Microscopy (SNOM).
Image contrast: Depends on the type of tip – sample interaction.
3. **Resolution:** Sub-Å resolution possible. Not determined by diffraction effects but only by the tip-sample interaction as well as by the radius of the scanning tip. Atomic resolution is obtained only for clean and well prepared sample surfaces and SPM tips.
4. Different **scan modes exist**: Constant height, constant interaction, DC / AC interaction modes, hybrid modes. **3D topography reconstruction** by constant interaction mode.
5. **Feedback loops** of the SPM systems use a **Proportional – Integral – Derivative control system** to minimize the error signal of the detector and to regulate the tip-sample distance during the scanning process.

Appendix

Literature and History of Scanning Probe Microscopy

1. **Scanning Probe Microscopy**, E. Meyer, H.J. Hug and R. Bennewitz, Springer Verlag (2004).
2. **Scanning Probe Microscopy and Spectroscopy**, R. Wiesendanger, Chambridge Univ. Press (1994).
3. **Noncontact Atomic Force Microscopy** S. Morita, R. Wiesendanger and E. Meyer, Springer (2002).
4. **Introduction to Scanning Tunneling Microscopy**, C.J. Chen, Oxford U. Press (1993).
5. **Scanning Tunneling Microscopy**, eds. J. A. Stroscio and W. J. Kaiser, Methods in Experimental Physics, Vol. 27, Academic Press (1993).
6. **Scanning Tunneling Microscopy and its Applications**, Chunli Bai, Springer (1992).
7. **Scanning Tunneling Microscopy and Spectroscopy**, D. A. Bonell, VCH (1993).
8. **Raster Tunnel Mikroskopie**, C. Haman und M. Hietschold, Akademie Verlag (1991).
9. **Scanning Tunneling Microscopy I - III**, eds. R. Wiesendanger and H. J. Güntherrodt, Springer (1994).
10. **Nanoscale Characterization of Surfaces and Interfaces**, N. J. DiNardo, VCH Verlag (1994).
11. **Scanning Force Microscopy with Applications to Electric, Magnetic and Atomic Force**, D. Sarid, Oxford Univ. Press (1992).
12. **Near Field Optics: Theory, Instrumentation and Applications**, M. Paesler and P.J. Moyer, John Wiley (1996).

Review articles:

13. **Scanning Tunneling Microscopy and Related Methods**, eds. R. J. Behm, N. Garcia and H. Rohrer, Kluwer Academic Press (1990).
14. **IBM Journal of Research and Development**, Vol. 30/4 (1996).

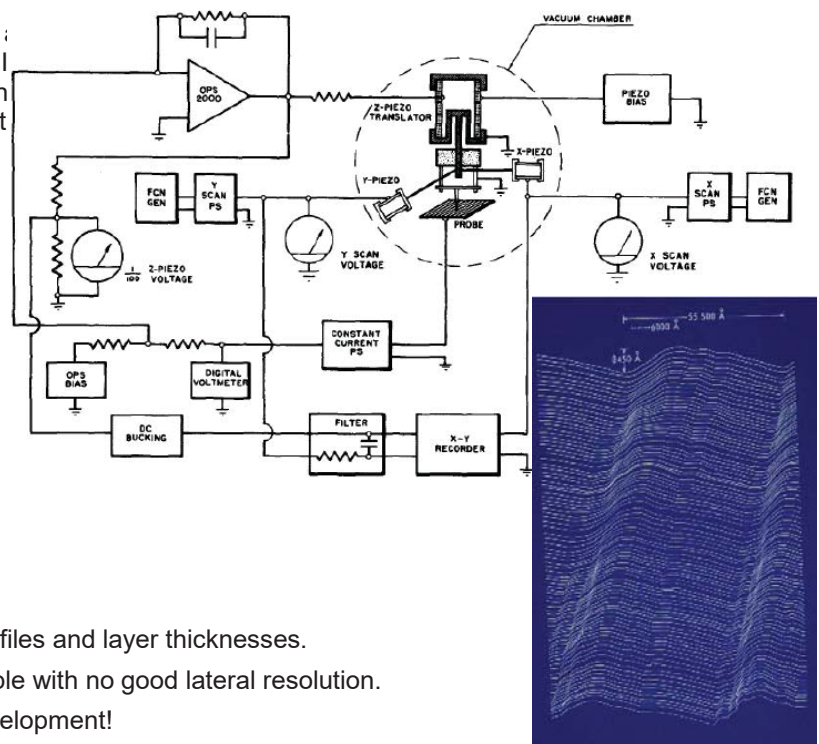
The History of Scanning Probe Microscopy

(i) Forerunners

- **Topographiner** (R. Young et al., NIST, 1972):
Microscope measuring the field emission from : tip to a sample at a distance of several 100 Å. I scanning mode, lateral resolution of about 20 nm and of ~3 nm in vertical direction. Problems with mechanical instabilities.



Russell Young, John Ward, and Fredric Scire



- **Stylus-profilometer** for measuring surface profiles and layer thicknesses.
Mechanical scanning of a hard tip over a sample with no good lateral resolution.
But: No significant influence on the further development!

(ii) Invention of the scanning tunneling microscope

by **G. Binning** and **H. Rohrer** (IBM Research Lab in Rüschlikon, CH) together with C. Gerber and E. Weibel).

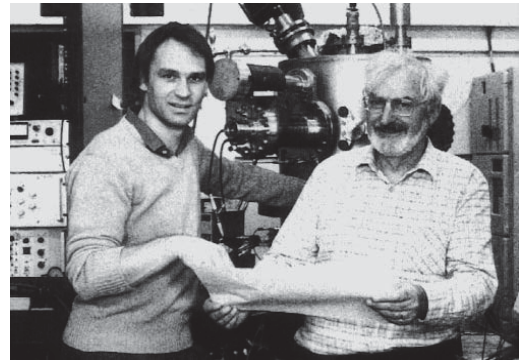
Original research direction (starting 1979):

Aim: Local tunneling spectroscopy of thin oxide layers to overcome the problems caused by inhomogeneous thickness and defects in MOS oxide layers used in semiconductor devices.

Task: Develop an instrument based on the idea of vacuum tunneling through a very thin gap between the probing tip and the sample.

In order to be able to record tunneling spectra at different position on the surface, a means to position the tip laterally on the surface was required.

=> Scanning the tip over the sample immediately resulted in the possibility to obtain information on the sample topography and thus to use this instrument for microscopy !

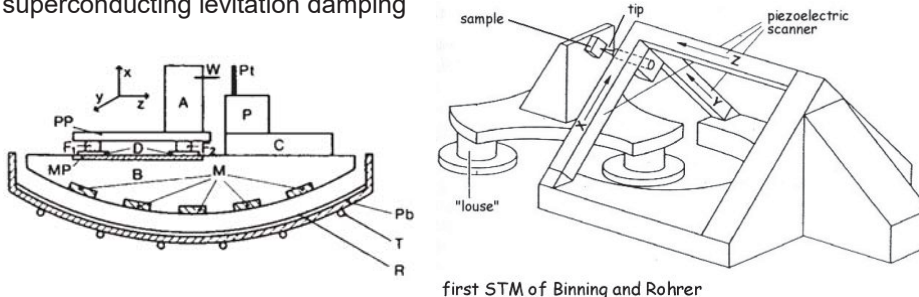


Problems that had to be solved:

- ❖ Sub-Å stability of tunneling gap against **mechanical vibrations** from the surrounding environment
» solved by rigid mechanical design of STM head and by spring suspension and eddy current damping,
- ❖ **movement and positioning** of the tip over the sample with sub-Angstrom precision,
» solved by using **piezoelectric positioning elements**,
- ❖ macroscopic and well-controlled **approach of the tip** and sample into the Å regime where a tunneling current appears: » solved by "louse" walker
- ❖ **Preparation of sharp and clean STM tips** and clean surfaces: UHV system

Instrumental developments by Binning, Rohrer, Gerber und Weibel:

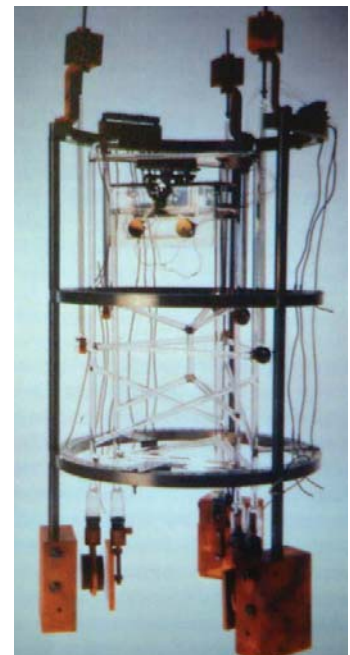
First (not working) prototype: low-temperature STM with superconducting levitation damping



first STM of Binning and Rohrer

After 2 years development time:

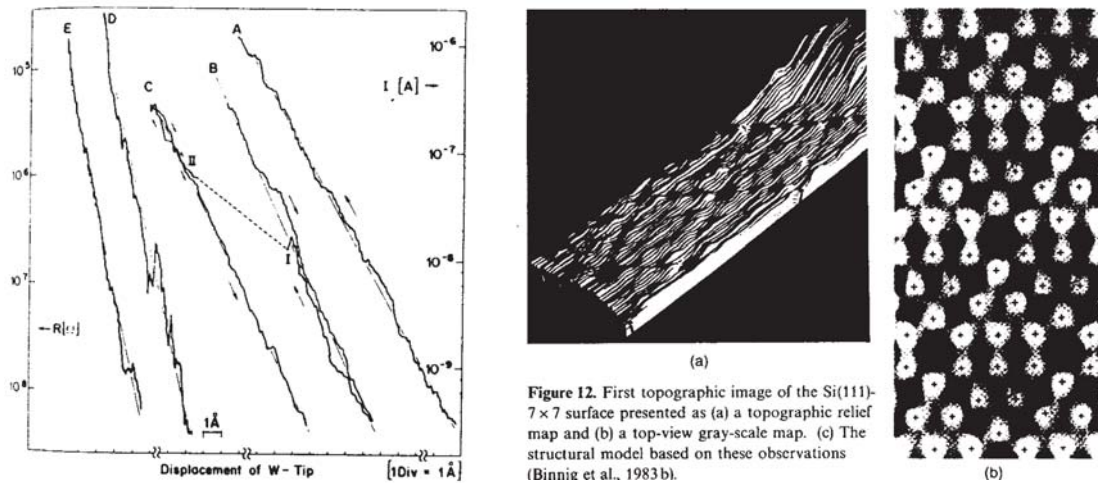
1981: first UHV compatible STM system with spring suspension



1981: First well-defined tunneling measurements (see Fig. below) of exponential dependence of the tip-sample current versus distance during the night time.

First topographic images of surfaces with resolution of single **monoatomic surface steps** (Gold (110) and CaIrSn_4 (110)) but no lateral atomic resolution.

First atomic resolution for 2x1 reconstructed Au(110) surface (unpublished) but measurements still unstable



Okt. 1982: Breakthrough with resolution of the atomic structure of Si(111) 7x7 surface reconstruction.

Additional experiments: Atomic resolution of the O_2 - induced (2 x 1) reconstruction of the Ni (110) surface and of the (2 x 2) reconstruction of the Ni(100) surface, surface reconstructions of Au and of Au on Si (111).

1983: First STM imaging of DNA chains.

1985: After three years, **other research groups** could also achieve atomic resolution by STM.

- F. C. Quate et al. (Stanford): Pt (100) 1 x 1 surface,
- R. Feenstra et al. (IBM, USA): cleaved GaAs(110) surface.
- P. Hansma et al. (Santa Barbara): graphite,
- J. Golovchenko et al. (Harvard): Ge on Si (111).

⇒ This finally lifted wide spread doubts on the results of G. Binnig and H. Rohrer and was the **final breakthrough of STM**. Immediately the first conferences and workshops on STM were started with rapidly increasing number of participants and presentations as well as of publications over the years.

⇒ Also: Scanning Capacitance Microscope (1984) and Scanning Near-Field Optical Microscope (1982).

1986: Nobelprize to G. Binnig and H. Rohrer for invention of STM.

1986: Invention of the **atomic force microscope** Binnig, Quate and Gerber (in Stamford) with "quasi" atomic resolution.

1987: Non-Contact AFM, Magnetic Force Microscope, Scanning Frictional Force Microscope,

1986: Surface modification and lithography using SPM methods by: mechanical indentation, local oxidation, tunnel current exposure, local deposition, local charge storage, etc. . feature sizes down to 1 nm.

1988: Ballistic Electron Emission Microscope, Scanning Electrochemical Microscope, Scanning Ion Conductance Microscope, Scanning Kelvin Probe Microscope, Scanning Thermal Microscope, Phase Detection and Force Modulation Scanning Force Microscope. etc. .

1988/89: Foundation of **first companies** for commercialization of STMs & AFMs: Digital Instruments and Park Scientific Instruments both in California (USA).

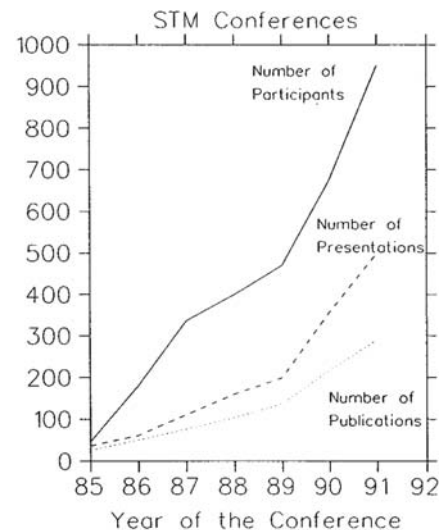
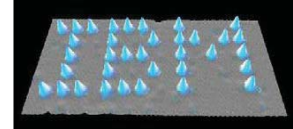
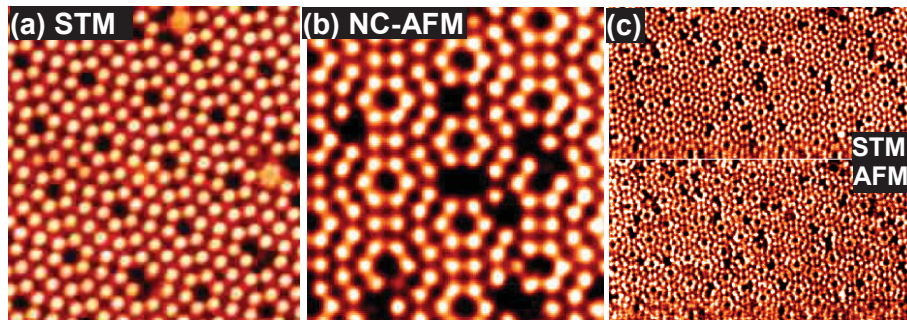


Fig. 0.3. Statistics of STM conferences between 1985 and 1991. Plotted are the number of participants, the number of presentations and the number of publications in the STM conference proceedings.

1990: Manipulation of single atoms of Xe on Ni (110), Eigler&Schweitzer (1990, IBM)

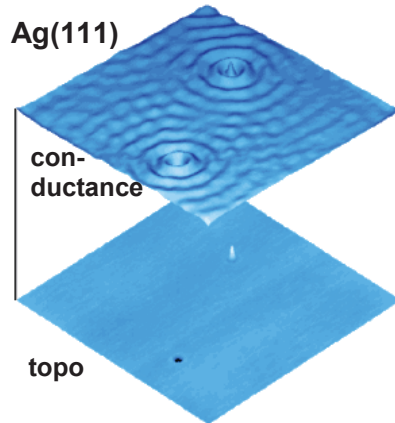


1996: True atomic resolution with AFM demonstrated for Si (111) by Giessibl et al.,



Example: Atomic Resolution of Si(111) 7 x 7 in UHV

- (a) STM: $U = 2 \text{ V}$, $I = 2.0 \text{ nA}$,
- (b) Non-Contact Mode AFM,
- (c) Multi-mode operation: simultaneous measurement of the topography in STM mode using a conductive cantilever, and of the atomic scale variation of the force, i.e. cantilever deflection.



1993: Imaging of Surface Electronic Wave Functions

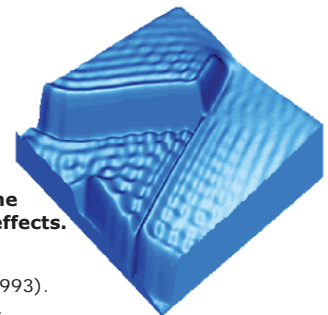
Example: Surface State Waves on Ag (111) at T=5K

Standing surface state waves around two surface defects on a Ag(111) film grown on HOPG imaged with LT STM at T = 5 K in the constant-current mode.

Left images show the standing waves (**upper image**) and the topography (**lower image**). The hole defect and the adatom defect lead to distinct differences in the centre of the two circular waves which exhibit pronounced interference effects.

References :

1. M. F. Crommie, C. P. Lutz, and D. M. Eigler, Nature 363, 524 (1993).
2. Y. Hasegawa and Ph. Avouris, Phys. Rev. Lett. 71, 1071 (1993).
3. J. Li, W. D. Schneider, and R. Berndt, Phys. Rev. B. 56, 7656 (1997).



Present Day Status

~20 different commercial producers of SPMs:

Omicron (D), Oxford Instruments (UK), RHK Technologies (US), Burleigh Instruments (US), Digital Instruments/Veeco/Bruker (US), McAllister (US), Zeiss (D), Melles Griot (F), Asylum research (CA), Molecular Imaging (Arizona), NT-MDT (Russia), Pacific Nanotechnology (CA), JEOL (Japan),

Frequent mergers and take-overs:

Bruker = Veeco + Digital Instrument + ThermoMicroscopes + Park Scientific Instruments + Topometrix,

Annual revenues: ~ 200 Mio €/year; corresponds to ~1000 SPM,
number of instruments worldwide ~10.000 SPMs.

Application areas:

- **Research and development:** Physics, chemistry, material science, biology, medicine, mechanical and electrical engineering in universities as well as industrial research labs and production.
- **Materials:** Semiconductors, ceramics, metals, magnetic materials, polymers, bio-systems, soft matter, Industry: semiconductor and microelectronics industry, CD and magnetic data storage industry, optical industry, coating industry, materials, chemical and pharmaceutical industry, medical diagnostics, hospitals,
- **Nanotechnology:** Nanoanalysis and Microscopy, Nanofabrication and Manipulation,